Review of ‘Probabilistic forecast using a Lagrangian sea ice model: application for search and rescue operations’ by Rabatel et al.

J.-F. Lemieux (Referee)

jean-francois.lemieux@canada.ca Received and published: 14 November 2017

First of all, we would like to thank the referee for his in-depth review of the manuscript and his numerous and relevant comments and suggestions. Please find below the answers in blue text to each of the points raised.

NOTE: *In the revised manuscript, we added few words about how we proceeded to optimise the air drag coefficient for the free-drift model, and indicated which value we found. We also updated all the figures showing the results of the new FD simulation and changed the text when describing the results accordingly. Note that it does not change the conclusions of the paper, but modify quantitatively the results we obtain, especially making FD and neXtSIM more similar in the summer.*

title suggestion: Probabilistic forecast using a Lagrangian sea ice model: impact of rheology

We changed the title following your suggestion to:
“Impact of rheology on probabilistic forecast of sea ice trajectories: application for search and rescue operations in the Arctic”

1. Major comments

1) You need to give more details on how you initialize the forecasts. Do you use fields (h, hs, A, d, u) from the previous forecast? And how do you deal with the FD model? I guess you use the thickness field from neXtSIM as the thickness field from a model without rheology would be completely unrealistic. Please relate that to the caption in Fig. 6.

Thanks to your comment. Yes indeed, we completely missed to provide explanations on the initial conditions. We use fields from previous neXtSIM simulations on the same period with the same external forcings but without wind perturbations. The text has been updated accordingly (p.11 l.20 and p.12 l.1-2).

2) I understand why you neglect the rheology term for your FD model. However,

what is the justification for neglecting the inertial term?

When the rheology is not taken into account, the time scale of the ice dynamics is short (few hours) and the steady state solution (acceleration set to 0) is rapidly reached (see McPhee1980 and Lepparanta2005). Note also that for this study we wanted to use the simplest model as possible, for which an analytical solution can be easily calculated. This is also consistent with Grumbine 1998.

3) Fig 2. and p. 9 line 3: How do you define FD ’events’? Concentration threshold?

No concentration threshold here. A FD event is defined as the one when the simulated ice velocity is within a range of 10% around the value of the free-drift solution. By doing so, we avoid using any concentration threshold that can be somehow misleading or at least a poor constraint for defining region of free-drift. The text has been updated accordingly (p.10 l.12-15).

You have optimized C_a for neXtSIM. Your conclusion (p. 23) says you have done the same thing for the FD model. This should be mentioned and clarified earlier. I also suggest you give the C_a value you obtained for the FD model.

Thanks to your comment, we realised that the way we optimised the drag coefficient for the free-drift model was not optimal because it used the same geographical restriction as for the neXtSIM model. We therefore re-optimised that parameter for FD, without applying any geographical restriction. Then we re-ran the free-drift simulations for both winter and summer with the newly optimised drag coefficient.

In the revised manuscript, we added a short explanation on how we optimised the drag for the free-drift model, and reported on the optimal value we found. We also updated all the figures relative the FD simulation and changed the text describing the results accordingly. Note that, the use of the new (optimised) drag coefficient does not lead to changes in the conclusions of the paper, yet it modifies quantitatively the results we obtain, especially for the summer.

4) You often discuss spatial correlations between certain fields (e.g. Fig 7 and 8). You relate these high correlations to the rheology and the thickness field. I think it would be a good idea to show maps (winter and summer) of the effective elastic stiffness as it is more representative of the 'strength' of the ice cover than just the thickness field.

We choose to show the map of ice thickness because, after the concentration, this is the quantity that correlates the most with the drift response to external forcing, and has the advantage of being a meaningful physical variable to everyone. In winter for instance, the concentration is close to 1 everywhere and it is therefore unable to display any spatial correlation (if any). We agree with you that the elastic stiffness is more representative of the "strength" of the ice cover, in a mechanical sense. Nevertheless, except locally (along the LKFs) where the ice is highly damaged, the geographical pattern of elastic stiffness is at first order correlated to the thickness pattern, and have thus opted to show the latter in view of its clearer physical meaning.

I am also wondering what is the effect of the pressure term? My impression is that the effective elastic stiffness gets very small in summer because the ice is so damaged and cannot heal so that the pressure term plays an important role.

The pressure term is large only when the local deformation is convergent and if the concentration is close to 100% (See equations 17 and 18 in Rampal et al. 2016b). In summer, it is correct to say that there is no damage healing, and therefore damaged sea ice can only loose mechanical strength over time.

5) In the comparison of the predictive skill of the model with and without rheology, you look at the error of the barycenter. I think you could also discuss whether the error e(t) of the barycenter is smaller than the one of a single deterministic forecast (no perturbation to the wind). Even if it is not the case, the probabilistic forecasts with its spread would still give important information...

Indeed, this is a good suggestion. The comparison with the deterministic forecast does provide important information. We have re-run our model to get the deterministic "forecasts", using the ASR reanalysis as forcing and the air drag coefficient equal to 0.0065 (after optimisation with OSI-SAF *dataset). We find the forecast error from a single deterministic forecast is close to the probabilistic barycenter, especially in winter, but is larger by 15% in the summer, so there is a small benefit of using the ensemble mean of a probabilistic forecast. Looking at the barycentric coordinates (e_para and e_perp), we note larger differences in the parallel components, whereas the perpendicular components are similar (see Fig. 15 in the revised manuscript).*

I would also be curious about the following experiment...what happens if you move your virtual buoys with the persisted initial velocity of the observed buoys (see Hebert et al. 2015). At what lead time is the ensemble of neXtSIM better than the persisted observed initial velocity? I guess this could give you some indications about the quality of your forcing field.

While we agree with the Reviewer that the comparison with a persistent forecast could be an interesting experiment to perform, we consider it slightly out of the scope of this work that is centred on the impact of rheology. We hope to be able to investigate this further in the future.

2. Minor comments

1) Overall the english and the text is very good. There are a few typos. Here is a list of some of them: p.1 line14, p.4 line4, p.11 line29, p.20 line5, p.22 line29, p.25 line28.

Done

2) p.2 line 5: Add ’sea ice’ before ’forecasting systems’.

Done

3) p.2 line 5: Note that RIPS is no longer in operations and has been replaced by the coupled Regional Ice Ocean Prediction System (RIOPS). It would be better to rephrase. The references for this new system are Lemieux et al., 2016 (the paper you already cite) and Dupont et al. 2015: A high-resolution ocean and sea-ice modelling system for the Arctic and North Atlantic oceans.

Thank you for your note. We updated the name of the prediction system to RIOPS, and we added Dupont et al 2015 as a reference.

4) p.3 line 3: remove ’advanced’...Just say what it is.

Done

5) p.3 line 9: Coon et al., 1974 modeled sea ice as an elasto-plastic material...please rephrase.

Done

6) p.3 line 18: ’sea ice responds in a linear way’ is vague. Please clarify what you mean by that.

Done

7) p.3 line 20: You could add ’(due to the limited number of observations)’ at the end of this sentence.

Done

8) p.3 line 27: Change ’full complexity of the present version’ by ’the latest model developments’ .

Done

9) p.4 line 9: Change ’spatial’ by ’spatially’.

Done

10) p.4 line 20: Change ’refreezing’ by ’freezing’.

Done

11) p.4 line 23: What do you mean by ’effective’? Grid cell mean values?.

Yes, you are correct. The unit of the effective thickness is a volume per unit of area.

12) p.4 eq. 2: I am not familiar with this formulation of the vector product for the Coriolis term...Don’t you want to use the common formulation with the ’x’?

Yes indeed, we changed the notation.

13) p.6 line 8: Add ’virtual’ before ’buoy’.

Done

14) p.6 line 20: I think you need to divide by N in the equation for B(t).

You are correct. Thank you for having spotted this typo which is now corrected.

15) The second figure you refer to is Fig.4 (p. 8 line 4). Please change the order.

Done

16) p. 8 line 5: Are these 10 m winds? Please specify this and mention the turning angle you use (maybe also for the ocean currents).

We use turning angles of 0 and 25 degrees for the air and water drags, respectively. These values are now listed in a table that we added in the revised version of the manuscript and in which all the parameters are reported with their respective values. Note also that these values are the same as those used in Rampal et al. 2016b.

17) p. 9 line 3: Remove ’state-of-art’...Just say what it is.

Done

18) p. 9 line 17: ’Dominant’ is a bit confusing here because it sounds like it is the largest term in the momentum equation (the wind stress is usually the largest one). Please rephrase.

Yes, you are right. The word "dominant" is not the right one. We now have rephrased the sentence (p.11 l.11).

19) p. 10 line 3-5: Why are thermodynamics an issue? You have a thermo model, right?

There must be a misunderstanding here. The thermodynamics is indeed not an issue. We indeed use a zero-layer thermodynamics model (Semtner, 1976) to melt or form new ice, as well as for the damage healing.

What we intended to explain therein was that, in order to ensure a fairer comparison between the free drift model and a model with sea ice rheology, one need to make sure that the sea ice thickness/concentration fields during the simulation is as realistic as possible. This is not the case with the free drift model that, by definition, does not limit the amount of ridging for instance, leading to unrealistic thickening and consequent degrade of the forecast performance in terms of drift. We modified the text accordingly (p11. l.16-20).

20) p. 10 last line: Add 'steady state' before 'drift'.

Done

21) Fig.5: It is difficult to see the coherency between the neXtSIM panels because the lower panel is almost only blue. Can you improve the colorscale so that we can see better the difference? (same idea for Fig. 7)

We choose this colorscale in order to highlight the quantitative differences between mu_b in neXtSIM and FD. Indeed, in this case, the neXtSIM panels become very blue, especially in winter. We changed the colorscale as suggested in order to highlight the pattern.

22) p. 11 line 25-30: You mention correlations between spatial fields. Is it just by looking at the figures or you actually calculated spatial correlations?

This is only a qualitative visual evaluation based on looking at the figures and checking for common patterns. In our case, we considered the correlation looked obvious.

23) p. 14 line 1: Clarify what you mean by 'the response'...ice velocity? 4

The response in terms of period averages of mu_r and mu_b. We updated the text as suggested.

24) p. 15 line 3 and elsewhere: Is 'on another hand' a correct expression? Is it better to use 'on the other hand'?

Thanks, We did change the text as suggested.

25) Fig. 13: How do you define the mean sea ice coverage (A=15% contour)?

Actually, the grey area shows the presence of the sea ice at least during 10 consecutive days (the length of simulations) during the winter or summer period. We added a sentence in the caption figure to clarify this point (Fig.14).

Looking at these two panels, as all the buoys are in regions of thick compact ice, it is kind of obvious that neXtSIM will do better than FD in this experiment. In other words, the FD model would do better if the buoys were uniformly distributed. I would add a sentence to mention that.

This is correct. We added a sentence as suggested (p.20 l.9-13).

26) As you calculated the POC for Fig. 17, I suggest you give the exact definition of the POC in eq. 13 instead of saying that it is proportional to...

This is a good suggestion. We added a sentence with the exact definition of the POC (p.22 l.13-14).

27) Fig. 17: same idea as before, what happens if you use the deterministic forecast instead of the barycenter? Do you get a real benefit from the ensemble forecast for the time evolution of the POC?

As explained before: we re-ran deterministic forecasts, using the ASR reanalysis as forcing and the air drag coefficient equal to 0.0065 after optimisation. We obtain similar POCs from ellipses centred on the deterministic forecast (black lines) in winter, whereas they are smaller in summer (see Fig. below).

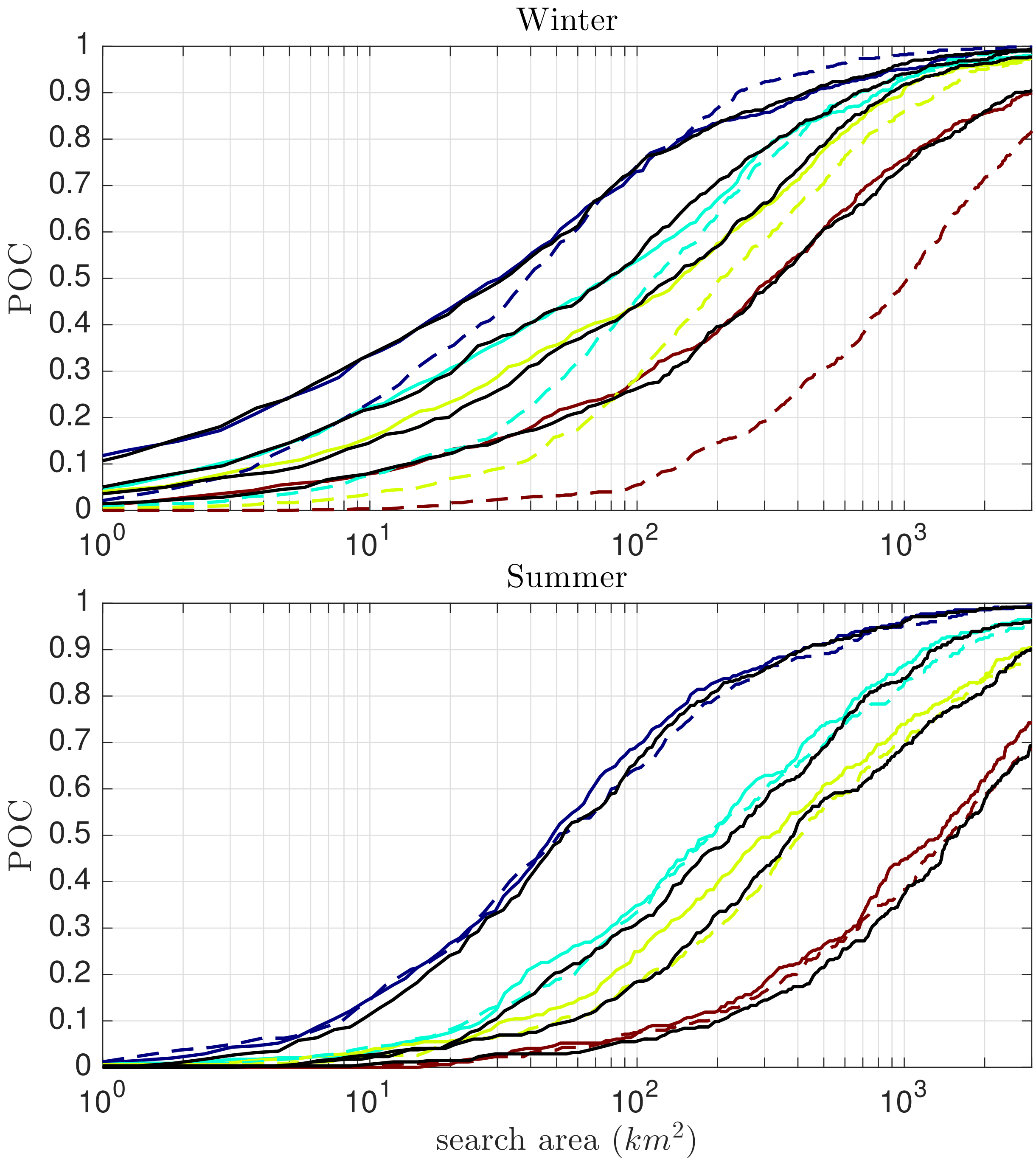

28) Please rephrase the last sentence of p. 22.

Done

29) p. 23 line 3: replace ’sensitivity’ by ’sensitive’.

Done

30) p. 25 lines 7-9: I understand what you mean but I find that the two sentences (’Still it is the wind...’ and ’we suggest instead...’) kind of contradict each other. If the wind is the key player, efforts should be made to improve the forcing winds (by improving the assimilation and forecasts of

the atmospheric model). Just rephrase a bit. By the way I like the discussion about assimilating sea ice fractures...Interesting.

We agree that the sentence about the wind was confusing and in contradiction with the point we wanted to make. We therefore decided to remove that sentence.

Interactive comment on "**Probabilistic forecast using a Lagrangian sea ice model: application for search and rescue operations**" *by* **Matthias Rabatel et al.**

H. F. Goessling (Referee)

First of all, we would like to thank the referee for his in depth review of the manuscript and his numerous and relevant comments and suggestions. Please find below the answers in blue text to each of the points raised.

NOTE: *In the revised manuscript, we added few words about how we proceeded to optimise the air drag coefficient for the free-drift model, and indicated which value we found. We also updated all the figures showing the results of the new FD simulation and changed the text when describing the results accordingly. Note that it does not change the conclusions of the paper, but modify quantitatively the results we obtain, especially making FD and neXtSIM more similar in the summer.*

1) Concerning terminology, I think it would be worthwhile to clarify that this study is using the term "forecast" not in the sense of forecasting actual future trajectories, where the future evolution of the system is becoming more and more uncertain over the forecast lead time through chaotic error growth, but in a slightly different way where the future evolution of the most chaotic component - the atmospheric forcing - is approximately known. Of course uncertainties are introduced in another way, namely through perturbations of the atmospheric forcing, but still the underlying synoptic evolution is the same in all ensemble members. I'm not trying to say that this is not worthwhile doing; in particular, one can imagine search & rescue applications where one aims to find the current position of a target that got lost 10 days ago, so one could run a "forecast" system like the one used here to "nowcast" the current position using near-real-time atmospheric (re-)analyses. And, obviously, one could also use actual atmospheric forecasts to drive the model, but that is not done in this study, so I recommend to just clarify this.

Agree, we specify in the introduction that we work in the context of a "hindcast-forecast" with analysed atmospheric forcing, which error uncertainties are emulated as representative of forecast errors. In the context of data assimilation, this procedure is akin to the propagation step of Ensemble Kalman Filter for generating "forecast" error covariance matrices (which should also be called "hindcast-forecast" to be precise).

2) P2L33: "departing from independent in situ drifting buoys, and compare them with real observations"; Does "in situ drifting buoys" not refer to the "real observations"? Please clarify.

Thank you for your comment. No indeed, we replaced the not suitable term: "in situ" by "virtual".

3) P3L28-29: "the impact of some mechanical parameters on the ice deformation can still be considered as valid"; the "some" sounds very vague, could you be more specific?

Yes indeed. Actually, all mechanical terms are involved. We changed the text (p.3 l.32).

4) Eq1: If I am not mistaken, this holds only when h and hs are the "effective" (grid-cell averaged) thicknesses, correct? And for A it stops holding for A close to 1, in particular if there is a lot of damage where there can still be considerable convergence despite A=1 (even with the "pressure term"), right? This would deserve some clarification.

Yes, the h and hs are indeed volumes per unit of area and A is bounded to 1, even when ridging occurs.

5) Eq5: It may help to mention what value is used for alpha (probably -20 as in Rampal et al. 2016?) so the strongly non-lineas dependence on A becomes obvious.

Yes indeed, we used the same alpha value, i.e. -20, as in Rampal et al. 2016b. To make sure this is clear to the reader, we decided to add a table listing all the parameters of the model and the values used for our experiments.

6) P5L24-28: To me this paragraph sounds very vague; could the authors be more specific on what inputs and outputs are considered?

We removed that paragraph.

7) Eq8+9: It might be worth noting that the means of "b_i,II" and "b_i,L" are zero and thus omitted in Eq9. It might also be worth

pointing out that mu_b contains basically the same information as "b_i,II" and "b_i,L" (except the directional information); they do not relate to each other like the first and the second momentum of a distribution (which is not stated, but at least I was confused at first).

Thank you for your comment. Yes indeed, the means of b_i,|| and b_i,L are zero and highlight only directional information. However, as the directions are perpendicular, we use the sample standard deviation of these distances to define the anisotropy. Then, b_i,|| and b_i,L are no longer used in the paper. We rephrased the paragraph to avoid confusion (end of p.8).

8) Fig2: What data and analysis is this figure based on? And what temporal sampling frequency is used to detect "events", e.g., one day?

About events, the temporal sampling frequency used is one day. The ice velocities from these events are compared with the observed ice drift from OSISAF dataset. We updated the text accordingly.

9) P9L17: "the internal stresses in the ice, and the corresponding Grad(sigma h) term in Eq. (2), becomes very large and dominant"; Would it be more precise to say that it almost completely balances the other forces (so that the acceleration (and speed) becomes very small)?

Thanks for this suggestion. We rephrased the sentence to avoid confusion; the use of the word "dominant" was indeed not a good choice. This is now clarified in the revised manuscript (p11. l.11).

10) P10L6: "We ran an ensemble of 12 members, each of them forced by the perturbed wind dataset generated as explained above"; If I have not overseen some important detail, there is some information on the experimental setup missing. In particular, how are the sea ice and ocean in the different members initialised? Is there one single "reference run" from which the ensembles are brached off, with all members keeping the same initial sea-ice/ocean state? If so, does the reference run also have perturbations to the winds (and accordingly uses the re-tuned parameters)? Or are there just 12 simulations overall, covering the whole time period, so that the "initial" sea-ice/ocean states are different between the ensemble members? The latter doesn't seem to be the case as you speak of individual simulations in P10L3. Also, P25L5-6 seems to hint that indeed the initial states are identical. In any case I have the impression that the question of whether or not the initial sea-ice states are identical is very important for the interpretation of some of the results (see below), so I think this should be described very clearly.

Thanks to your comment: we completely missed to provide explanations on initial conditions. Indeed, all members are initialised with the same sea ice state coming from the reference simulation presented in Rampal et al. 2016b on the same period with same external forcings without wind perturbations. We have now added all the details regarding initialisation in the revised manuscript (end of p.11 and beginning of p.12).

11) P10L9: "8000 virtual buoy trajectories over the winter season"; Is this the number of ENSEMBLES of buoy trajectories? For individual trajectories I would expect a larger number, given the approximate number of initial positions in Fig4 and the number of 10-days periods.

You are right. It was confusing in the text, we updated the text stating the total number of trajectories (12 times greater).

12) Eq11: While you can certainly say that the omitted pressure term, as the stress term, belong to the rheology, the omitted tau_b could also be mentioned.

Yes, this is a good point. We updated the text accordingly (p.12 l.13).

13) P10L19: "The FD model therefore mimics the drift of a buoy at the surface of the ocean."; I would think that this is not really the case because the drag coefficients would be quite different (in particular on the water side due to turbulent momentum transfer between deeper layers and the surface water surrounding the buoy)?

Correct, a buoy in the open ocean would experience a different ocean drag. We use the term « mimics » for the sake of the analogy, given that The free drift case is analogous to the pure Ekman drift case in ocean dynamics. We have rephrased the text to avoid the confusion (p.12 l.16).

14) Fig5+7: i) I do not understand why the sea-ice thickness pattern is so clearly visible in the dispersion strength (mu_b) for the free-drift model where the rheology shouldn't play any role; could the authors comment? ii) I suggest to use the same colour scales for the two bottom panels so that the difference in mu_b becomes even more obvious

i) This is because the free drift model (eq. 11) takes into account the ice mass via the Coriolis and gravity force *terms. The thickness patterns, which are used as initial conditions and which are the same as in the corresponding neXtSIM simulations, are therefore reflected on both the advective and dispersive response of the FD model.*

ii) We tried to use the same colorscale for FD and neXtSIM but in this case, on one Figure of them (either FD or neXtSIM), one cannot see any pattern anymore. Finally, we choose to leave different colorscales in order to discuss on mu_b pattern (see Fig. below).

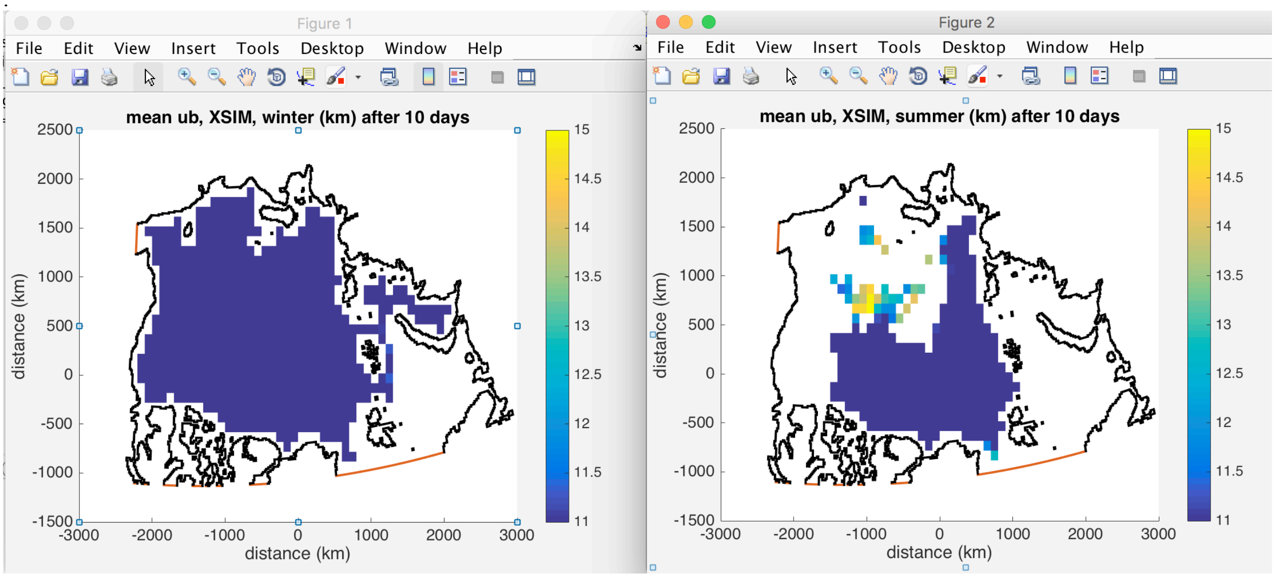

15) P14L1: "In both winter and summer, the response to wind perturbations is overall lower by 35% in neXtSIM than in FD"; Where does this number come from? I would have thought that the difference of mu_b in neXtSim versus FD would quantify "the response to wind perturbations", but those are reduced by 63% and 39% in winter and summer,

respectively (as stated in P14L5-6), so that doesn't fit. Could you please clarify? (Also at the beginning of Sect.5)

Thank you for your comment. Actually, this number was a global mean over both periods and both distances, but we removed it and changed the sentence.

Yes indeed, the distance b provides quantitative information on the response to wind perturbations. In summer, the reduction shows the behaviour of neXtSIM is closer to FD. This may be explained by the fact that, in summer, the ice concentration is reduced leading to a significant decrease of the internal stresses within the ice (p.13 l.23-32).

16) P14L21-27: Is the assumption correct that the values found for the ratio mu_r/mu_b should scale with the strength of the wind perturbations? If so, this might be worth mentioning.

It is an interesting assumption. Besides that, we studied this ratio on different ways: looking at the spatial pattern and the time evolution. However, we could not highlight any relevant correlation with wind perturbations and/or physical quantities. This ratio is roughly driven by mu_r and is not directly related to the wind perturbations.

17) P15L8-9: "This reveals that the ice will first tend to move compactly along the wind direction away from the origin, but it then starts to break and depart from the barycentre"; First, the wind directions felt by the different ensemble members differ instantly after the initialisation, right?

You are right.

18) So, moving compactly along the wind direction would imply a slightly different direction for each member from the very beginning. Second, the ice is "broken" (i.e., has fractures) already at initial time, right?

You are right, the initial damage is taken from the outputs of simulations used in Rampal et al. (2016b) for neXtSIM (not used in FD) and it is the same for all members.

19) Third, and maybe more importantly, I think that the interpretation of the decreasing anisotropy might depend strongly on the initial sea-ice state: Assuming that the sea-ice initial states are identical for all ensemble members, even slightly different winds will initially tend to drive motion in the same direction because the motion is strongly constrained by the pattern of fractures.

We agree with you.

20) Only after some time will the pattern of fractures differ between the ensemble members, and then the sea-ice motion fields will also be more different between the members. Could this not explain why the anisotropy is even larger at the beginning in neXtSIM and then goes down to lower values? This argument of course requires that the initial sea-ice states are identical, so that should be clarified.

You are right. We changed the text to highlight this valid interpretation (p18).

21) P16L11-13: "We found that the ensemble spread follow two distinct diffusion regimes, one for small time t«Gamma and one for large time t»Gamm where Gamma is the so-called integral time scale (Taylor, 1921), which is about 1.5 days for sea ice according to Rampal et al. (2009)"; Do I understand correctly that this integral timescale is quite directly determined by the autocorrelation timescale of wind anomalies or - in the present study - by the autocorrelation timescale of the wind perturbations? It might be worthwhile pointing out that this subtle difference exists between the present and the Rampal et al. 2009 study.

This is not true. The integral timescale can be influenced by the unperturbed winds and ocean forcing fields, the perturbations autocorrelation and (in the case of neXtSIM), the rheological model. Since the perturbations of the winds have an autocorrelation of 2 days, quite close to the limit of 1.5 days, it is unfortunately not easy to tell their effect apart from other effects, but we have not tried to add additional experiments for that matter.

22) P17L1-2: "Predictive skills" and "able to forecast real trajectories"; please see my general comment on the way the term "forecast" is used in this study.

We reminded the reader that this study is "in hindcast mode".

23) P15L12-14: "We observe that highest degree of ensemble anisotropy (R > 1) is found north of Greenland and Canadian Archipelago, where the ice is the thickest and the ice drift and winds the lowest, in overall agreement with the interpretation of the temporal evolution of R for neXtSIM in the winter"; There are also high values of R along the Eurasian and Alaskan coasts; can't this be explained by the fact that the sea-ice motion (and the associated dispersion) occurs mainly in parallel to the coasts because motion towards the coast tends to be suppressed by counteracting ice pressure (even when the thickness is moderate)?

Thank you for your comment; this is an interesting point. We agree with you and we updated the text accordingly (p18).

24) Fig11: For my taste it would again be better to use the same scale for all panels.

Unfortunately, with the same colorscale, either pattern of neXtSIM or FD will not be longer visible. We choose to keep different colorscale in order to exhibit the absence of spatial coherence for FD on the one hand, and on the other, the difference between ice coverage close to the coast and in the center of the domain.

25) Fig12: If I understand correctly, the slopes at lower timescales are all approximately 2. I suggest to note that also in the plot (as is done for the longer timescales).

Yes indeed. We updated the figure as you suggested (Fig. 13).

26) P19L10-11: "For FD, e_L still being positive for both periods, corresponds to a drift too far to the right in the observations"; What is meant by "to the right in the observations"? And is e_L for FD not NEGATIVE according to Fig14 right?

Yes indeed. This is an unfortunate typo, we corrected. The vector e is directed from the observation to the barycentre. Thus, standing on the observation and looking in the drift direction, a negative e_L corresponds to seeing the barycentre to the right (Fig. 15).

27) P21L10-13: "even if the forecast errors are smaller in neXtSIM than in FD, its shrunk search areas lead to a smaller POC for neXtSIM than for the FD model (not shown): in practice the probabilistic forecast from neXtSIM is too optimistic, underestimates the uncertainties in the forecast, while the FD forecast overestimates them"; First, I would in fact like to see a graph that shows how the spread (mu_b) versus the error evolves. In weather forecasting, the "spread-error relationship" is a common way to measure whether probabilistic forecasts are underdisperive ("too optimistic") or overdispersive ("too pessimistic"). The latter terms could be introduced also in the context of this study.

Thank you for your comment. We added a "spread-error relationship" graphic (Fig. 18 on the revised version) as you suggested. Actually, both models are underdisperive, however, where the spread is larger than 10 km, only neXtSIM seems become too pessimistic. We have added comments on this somewhat surprising behaviour (end of p.23).

28) P22L31-33: "The fact that most of the superiority of neXtSIM over reveals during winter is, as stated in previous instances, in full agreement with the expectations, given that during the summer the ice mechanics in the two models is similar"; Please check the grammar of this sentence.

Done. Hopefully improved.

29) Fig17: Could the superiority of FD at very short lead times and for large search areas (for which the skill of the barycenter is not important) be explained by the possibly too strong anisotropy of neXtSIM close to the initial time, due to the shared fracture pattern in all ensemble members (if the sea-ice initial states are indentical, see my previous remarks)?

Thank you for your comment. This is an interesting point. Indeed, when we define the search area as a circle (=without anisotropy), the POC from neXtSIM, for small time horizons and for large search areas, becomes greater than FD. For other time horizons, smaller areas and in summer, the difference is far less visible (see Fig. below). This means that the ensemble run is "too confident in its anisotropy", which could be improved with a better initialization of the ensemble. We added this note in the revised manuscript.

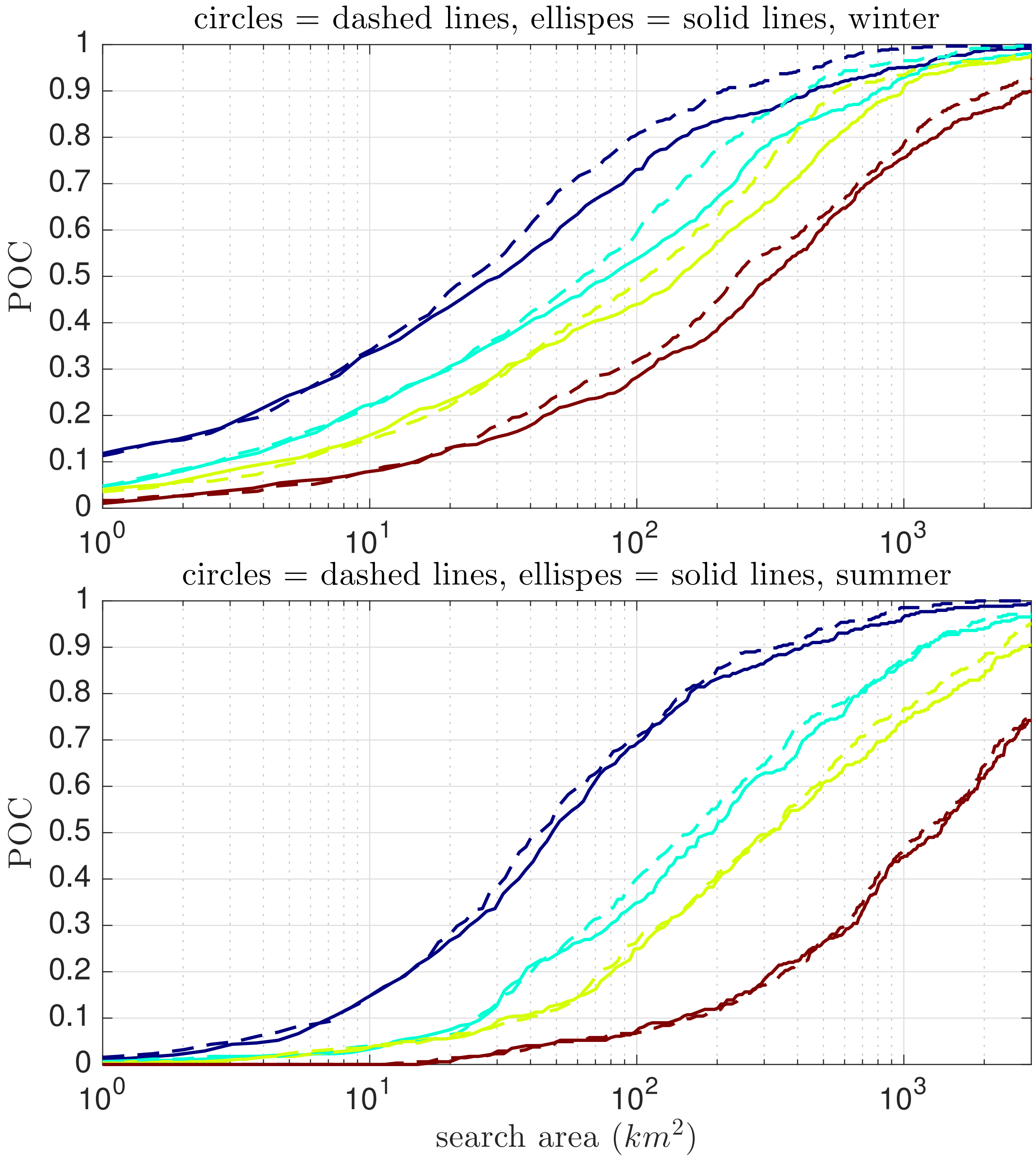

30) P24L7-8: “This mechanism is missing in the absence of rheology (like in the FD model) and represents a clear strength and advantage of the elasto-brittle rheology in neXtSIM”; Could the authors comment on what differences one might expect for other rheologies like the standard (E)VP?

We have noted some anisotropy in the EVP model in a previous experiment with TOPAZ (Bertino et al., 2015), which could unfortunately not be compared to the present results since it was not carried out in similar conditions.

Bertino, L., Bergh, J., and Xie, J.: Evaluation of uncertainties by ensemble simulation, Tech. Rep. Tech. Rep. 355, NERSC, ART JIP Deliverable 3.3, Bergen, Norway, 2015.

31) P24L18: "The model sensitivity to winds has been evaluated"; Wouldn’t it be more precise to say "The model sensitivity to wind perturbations has been evaluated"?

Yes.

32) P24L20-P25L1: "we are confident that the spread simulated by the model is physically consistent. Alternative sources of biases must be called such as, for example, other model inputs (thickness, concentrations, damage, ocean currents)"; Deficiencies to simulate reliable spread are commonly not referred to as "biases". Also, what does "must be called" mean here? Maybe in the sense of "must be mentioned?" And why to you refer to those model variables as "inputs"?

We significantly rephrase these sentences in order to clarify our discussions (p.28 l.23-30).

Technical corrections / comments

P1L6: "10-days" -> "10 days"

Done

P1L10: "in Arctic" -> "in the Arctic"

Done

P1L12: "to of free-drift model" -> "to the free-drift model"

Done

P2L33-34: "Without aiming to make it a key objective."; In terms of grammar, this seems to be an incomplete sentence.

Done

P3L7: "measures" -> "measurements"

Done

P3L8-13: Please check these lines for grammar (including commas).

Done

P3L19: "stands on the fact"; sounds strange.

Done

P3L31: "as follow" -> "as follows"

Done

P4L3: "Generalities"; I do not think that this term is commonly used this way.

Done

P4L4: "description neXtSIM" -> "description of neXtSIM"

Done

P6L10: "a initial position" -> "an initial position"

Done

P6L22: "explicit mention on the dependence" - "explicit mention of the dependence"

Done

P6L25: "informations" -> "information"

Done

P6L28: "Let consider" -> "Let us consider"

Done

P8L14: "the and the wind" -> "and the wind"

Done

P8L20-21: "ASR reanalysis" -> "ASR" (two times)

Done

P15L3: "On another hand" -> "On the other hand"

Done

P17L11: "average module"; ?

Done

P20L12: "all simulated ensemble of buoys" -> "all simulated ensemble members"

Done

P21L19: "can posed" -> "can be posed"

Done

P22L4: "models comparison" -> "model comparison"

Done

P22L5: "allow as also" -> "allow us also"

Done

P22L27: "larger of about" -> "larger by about"

Done

P23L7: "hold for" -> "hold also for"

Done

P25L18: "a elasto-brittle" -> "an elasto-brittle"

Done

P26L4: "founded" -> "funded"

Done

Review of “Probabilistic forecast using a Lagrangian sea ice model: application for search and rescue operations” by Matthias Rabatel, Pierre Rampal, Alberto Carrassi, Laurent Bertino, and Christopher K. R. T. Jones

First of all, we would like to thank the referee for his in depth review of the manuscript and his numerous and relevant comments and suggestions. Please find below the answers in blue text to each of the points raised.

NOTE: *In the revised manuscript, we added few words about how we proceeded to optimise the air drag coefficient for the free-drift model, and indicated which value we found. We also updated all the figures showing the results of the new FD simulation and changed the text when describing the results accordingly. Note that it does not change the conclusions of the paper, but modify quantitatively the results we obtain, especially making FD and neXtSIM more similar in the summer.*

General comments

The manuscript “Probabilistic forecast using a Lagrangian sea ice model: application for search and rescue operations” by M. Rabatel, P. Rampal, A. Carrassi, L. Bertino, and C.K.R.T. Jones provides a comprehensive evaluation of sea ice drift response to uncertainties in wind forcing using the sea ice model NeXtSIM with elasto-brittle rheology. The authors demonstrate through comparison with what is referred to as a free-drift model anisotropic behavior associated with sea ice mechanical properties in winter, with implications for predictive skill. This paper presents novel concepts and tools to highlight the importance of characterizing sea ice mechanics and rheology for such applications as search and rescue operations in winter. It is recommended that this manuscript be accepted for publication, following consideration of aspects including systematic error in NeXtSIM as documented in earlier studies of this Lagrangian sea ice model, spatial variability in the air drag coefficient, boundary condition sensitivity studies, and further investigation of reasons for discrepancies in dynamics for modeled and observed trajectories. Please find below more specific comments for consideration.

This is also to express agreement with the comments of both reviewers on the quality of manuscript, in addition to statements in regards to justification for term selection in the free drift model, and the need for further description as to how the forecasts are initialized.

Specific comments

Introduction

1) p. 2, line 28. In Rampal et al. (2016b), the authors show systematic errors based on comparison of simulated ice drift with the GlobICE dataset (Figure 7). Perhaps note in the Introduction, and provide a figure depicting, the spatial distribution of systematic errors for given timeframes in winter and summer, to distinguish from differences due to compactness and rheology based on comparisons between NeXStSIM and the free drift model. Highlight systematic errors based on comparison with OSISAF.

Thank you for your comment. We have added, in the introduction, a figure depicting the spatial distribution of systematic errors in winter. We do not provide the figure in summer since we do not consider the OSISAF data to be sufficiently reliable in this period (Fig. 1, p.4 l.1-5).

2) p. 3, lines 22 – 29. What parameter values are used in the present study, and in particular for compactness (i.e. as in Table 2 in Rampal et al., 2016b)? In the sensitivity analyses for the compactness parameter in Bouillon and Rampal (2015a) it is noted that the opening and closing rates are influenced by the compactness parameter. How are the current wind sensitivity results influenced by the choice of the compactness parameter?

You are right, we used the same compactness as in Rampal et al 2016b. A list of the values of the parameters was missing in our submitted manuscript. We have now added a table listing those in the revised manuscript.

In this study, we decided to restrict the sensitivity analysis to external parameters only, here the wind, and not to extent it to the internal mechanical parameters of sea ice like compactness, cohesion, etc. This choice is further justified by our mid-term goal of using neXtSIM in conjunction with ensemble-based data assimilation in which context the ensemble would preferably reflect the uncertainty on the external forcing under the assumption that internal parameters have all been already optimised.

We agree however with Reviewer on the relevance of such an analysis but we believe that it is beyond the scope of this paper, and it will be addressed in a different study.

Sensitivity analysis

3) Air drag coefficient and other parameters: Will there be regional variations in the drag coefficients?

There are no regional variations in this present study, both for the sake of simplicity and because constant drag coefficients are still customary in the community.

4) How is spatial variability in the drag coefficients addressed?

This is not addressed in the present study. We assume this coefficient to be constant over time and over the Arctic

5) Is the calibration method used the same as that in Rampal et al. (2016b)?

Yes, indeed. This is the same method used here. We explain it better in the revised manuscript, and also specify the values we obtain for neXtSIM and FD.

6) As previously noted, what value is used for the compactness parameter in this study?

We use the same one as in Rampal et al 2016b, i.e. -20.

7) Specifically: p. 9, line 2 and reference to the OSISAF dataset. Are similar results and values obtained for the air drag coefficient using the globeICE drift product for comparison, as in Rampal et al., 2016b?

We have not done any comparison to GlobICE in this paper as it is important for this specific study (and its goals) to perform the optimisation of the drag over the whole arctic, which would not have been the case if using GlobICE that has significantly less spatial coverage.

8) p. 9, line 6 and p. 8, Figure 2. Is concentration considered to account for spatial variability in the air drag coefficient, as described in Steiner (2001)?

As said before, we do not consider any spatial variability in the drag coefficient in this study. The concentration is actually not directly used to account for any spatial variability of the drag coefficient. But indirectly it is so, since we perform the optimisation only where the simulated drift is close to the free-drift solution, which *happens to be at locations where the concentration is significantly lower than 100%.*

9) In addition, what impact does the drag coefficient have on results?

Although this is an interesting question, this paper is not intended to address it. Still, between the submission and the present review, the drag coefficient of the FD model has been reduced from 5.1 e-03 down to 3.2 e-03, which has changed quantitatively the results in the summer but did not invalidate the conclusions.

10) p. 8, line 15. Perhaps provide justification for this wind speed variance selection (i.e. a value that is 6 times smaller than that used in Sakov et al. (2012).

Note that the value of 6 may sound dramatic while it only makes a factor of 2.3 in standard deviation. If taking the variance used in Sakov et al 2012, the impact on the neXtSIM behaviour is too large, i.e. the ice is breaking up too much leading to excesses of ice drift and very small anisotropy of the ensemble. We therefore decided to reduce that variance to a reasonable level so that the physics of neXtSIM can be expressed. In the future we will compare the relative sensitivities of the model used in Sakov et al. (2012) and neXtSIM.

11) p. 9, Figure 3. Is it possible to also identify and show systematic errors spatially in another panel in this or a separate figure? Please see previous comments for the Introduction.

See comment 1

12) p. 10, line 5. 100 km initial spacing. Are results and differences between the NeXtSIM and FD models influenced by different initial spacings?

We have not tested this.

However, if using e.g. 50km, we may not be able to consider anymore that a given drift trajectory of 10days is independent of each other as a given virtual buoy would sample more than one "box" over that period (average sea ice speed is about 6km/day in winter). So, taking 100km almost ensure that the trajectory members started from the centre of one box are independent of the trajectory members of the neighbouring box.

Results

13) p. 12, Figure 5. Should the contours for the lower panels be the same (i.e. <= 3 for both)? If not, perhaps emphasize the difference in diffusive spread spatial scales for the FD and NeXtSIM models since this, in addition to similarity in spatial patterns between minimum and maximum diffusive spread for both models is of interest and relevant to the present study.

We adjusted the colorscale as you suggested (Fig. 6).

14) p. 13, Figure 7. Similarly, the contour range should be the same. Sea ice dynamics are different for neXtSIM and FD even in summer. Perhaps include in the text a possible explanation for these differences (i.e. systematic error, parameter selection, FD characterization).

We tried to use the same color scale for FD and neXtSIM but in this case, on one Figure of them (either FD or neXtSIM), one cannot see any pattern anymore. Finally, we choose to leave different colorscales in order to discuss on mu_b pattern.

15) p. 14, line 15. '...effective elastic stiffness E depends non linearly on the ice concentration...'

Should this nonlinearity (and spatial variability) also be considered when optimising for the air drag coefficient? Should this too be considered with optimising for the air drag coefficient? Please see previous comments.

Such an optimisation of the drag where the rheology is active represents a complex non-linear inverse problem, highly sensitive to poorly known initial values (the ice damage and ice thickness among others). Our optimisation using free drift "events" is precisely intended to solve a simpler linear problem still using a sufficiently large number of observations.

16) p. 14, line 24. 'Where both (winds and ice thickness) are large, \gamma is large'. However, \gamma is also large in the southern Beaufort Sea for large winds and lower ice thickness in winter. Figures depicting maps of \gamma for the NeXtSIM and FD models in winter and summer would also highlight the impacts of ice rheology.

Thank you for your comment. Yes, indeed, both winds and ice thickness are not the only explanation. Perhaps, we may add: the sea-ice motion occurs mainly in parallel to the coasts because motion towards them tends to be suppressed by counteracting ice pressure. In summer, these coasts do no longer play the role of closed boundaries and the increase of R is almost no visible. This is corroborated by observing the pattern from FD where the pressure term does not interfere. We updated the text accordingly (end of p.18).

17) p. 15, Figure 9 caption. 'The PDFs for FD are similar for summer and winter...' Perhaps still show both PDFs in a separate panel with a different y-axis scale.

Thank you for your comment. We present this figure below. We believe it is not helpful to add it to the revised manuscript.

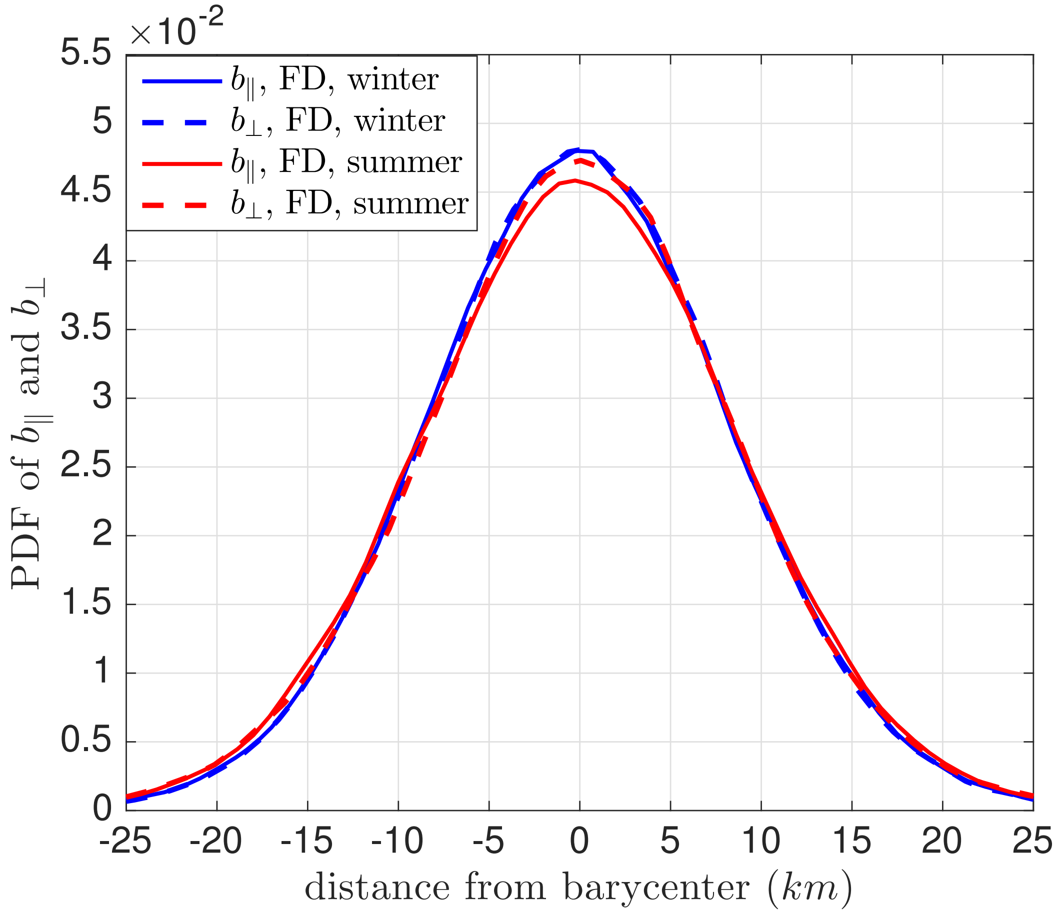

18) p. 15, lines 4 – 6. How are lateral boundary conditions (i.e. landfast ice and its extent)

addressed in the model? Would sensitivity analyses associated with boundary conditions highlight regional differences in anisotropy and preferential orientation?

We are not sure to well understand the question of the referee. However, here is our answer:

The lateral boundary conditions are either "free" (if at the ice edge) of "fixed" (if at the coast). If the ice cover does not extend anymore to the coast, the boundary conditions are therefore very different, and this likely has an impact at least over the peripheral band of ice near the ice edge. Further into the ice pack, the impact of the boundary conditions on the sea ice drift and anisotropy of the dispersion is less important. Local sea ice conditions (compactness/concentration and damage) are in this case more likely to be responsible for the anisotropy of the dispersion, which is what we discuss in our study.

As a conclusion, we do not think that performing sensitivity analyses associated with boundary conditions would reveal key information to understand the source of anisotropy of the ensemble spread.

19) p .16 and Figure 12. What are the possible reasons for discrepancies between the observed and modeled ice drift dispersion characteristics and temporal scaling exponents, namely the superdiffusive regime, in summer? Could superdiffusive behavior be attributed to other sources of uncertainty responsible for systematic error in the model?

We suggest that the super-diffusive behaviour we obtain for summer 2008 with neXtSIM, and which is in apparent contradictions with the results of Rampal et al. (2009) could rather be the fingerprint of a change in sea ice dynamical regime that occured over the most recent years, as a consequence of the thinner and more mobile sea ice cover . In this case, it would mean that the effect of the rheology became weaker (if not absent) in summer and that the sea ice response is now more directly related to ocean currents and winds, and therefore can exhibit super-diffusive behaviour as also reported in Lukovich et al. (2015). We modified the text accordingly (end of p.19 and beginning of p.20).

20) p. 17, Figure 11. Contour range should be comparable for the FD and NeXtSIM models. Is it possible to use the anisotropy ratio featured in Figure 11 to improve predictive skill for NeXtSIM?

Unfortunately, if we use the same colorscale, either one of the patterns of neXtSIM or FD will disappear. We choose to keep different colorscale in order to exhibit the absence of spatial coherence for FD on the one hand, and on the other, the difference between ice close to the coast and ice in the center.

21) p. 17, line 10. The forecast error vector components should be depicted accurately in Figure 15.

We updated the Fig. 15 (16 in the revised manuscript) as you suggested.

22) p. 19, Figure 14. How are **e**, **b**, and **a** related when considering the anisotropy ratio and is relation to forecast error? Variance in parallel and perpendicular components of b could also be compared with those for the forecast error in this figure or in figure 12 to demonstrate the anisotropic effects associated with elasto-brittle rheology.

The comparison of ensemble spread and errors on the same graph would not be helpful because the spread is underestimated by both models (see the new Figure 18). Also, note the answer to a related question (29)) from Reviewer #2, and the complementary graph below. The strong anisotropy may remain more of a hindrance than an advantage to search forecasting as long as the deformations are not assimilated in the model.

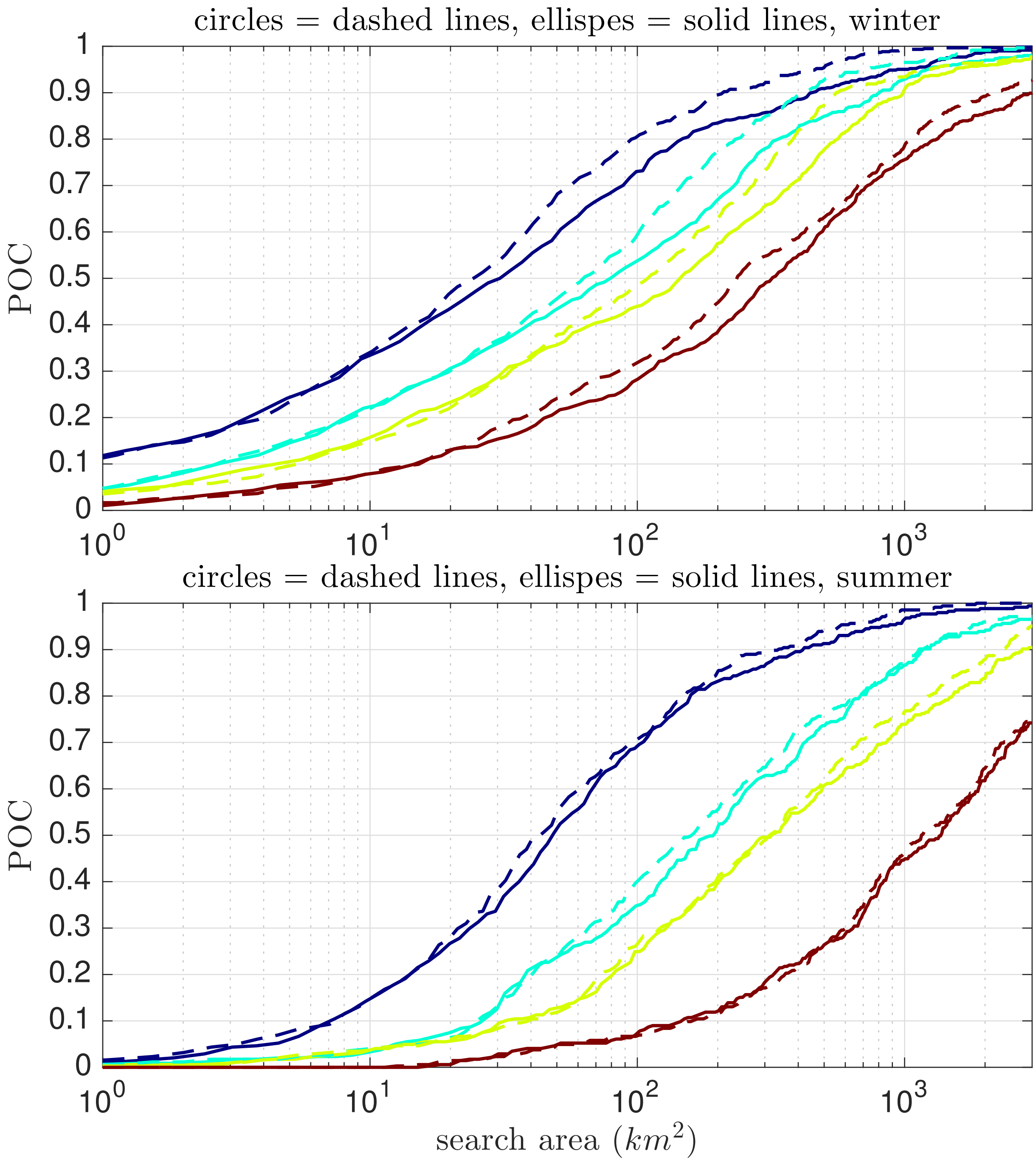

23) p. 21, line 19. 'for an equal area that can be searched' Does this imply for a fixed area?

Not fixed in the sense that the geometry is different (circle versus ellipse) the area included in the ellipse/circle is the same. Thus the sentence should be understood as: taking an ellipse (or circle) from either models with the same encompassed area, which of the two is more likely to contain the object? We have replaced equal by "a given area", hoping this will be clearer (p.25 l.5).

24) p. 25, lines 5 – 7. Would it be possible to quantify these contributions in additional sensitivity analyses?

The contribution of ice drift to the TOPAZ system with respect to other assimilated observations is quantified in Sakov et al. (2012) using the Degrees of Freedom for Signal. neXtSIM does not assimilate the same observations but the maps of μ_b in Figure 6 represent a sensitivity analysis of ice drift to spatially and temporally stationary perturbations of the winds.

Technical corrections

p. 1, line 12. Replace ‘of free-drift’ with ‘the free-drift’.

Done.

p. 2, lines 33 – 34. Combine the sentence ‘Without...’ with the next sentence.

Done

p. 4, line 10. Change ‘spatial’ to ‘spatially’.

Done

p. 5, line 24. Change ‘analysis’ to ‘analyses’.

Done

p. 6, line 25. Change ‘informations’ to ‘information’

Done

p. 7, Figure 1 figure caption. Perhaps replace ‘bouquet’ with ‘-member ensemble’.

Done

p. 11, line 25. Please change to ‘Chukchi’

Done

p. 11, line 30. Please replace ‘inn’ with ‘in’

Done

p. 14, line 14 ‘influences’

Done

p. 19, line 4 Replace ‘get very’ with ‘are’

Done

p. 21, line 19. Insert ‘be’ prior to ‘posed’

Done

p. 22, line 5. Perhaps replace ‘allow as also’ with ‘also allows’

Done

p. 22, line 27. Replace ‘of’ with ‘by’

Done

p. 22, line 30, Perhaps remove ‘up’

Done

p. 22, line 31, Perhaps replace ‘reveals’ with ‘FD is observed’

Done

p. 23, line 3, Replace ‘sensitivity’ with ‘sensitive’

We are used to seeing the wording “sensitivity experiment” rather than “sensitive experiment” which we interpret as an experiment dealing with a sensitive topic. So we would prefer keeping “sensitivity” (p.27, l.6).

p. 23, line 6, Replace ‘contrarily’ with ‘in contrast’

Done

p. 24, line 21, Replace ‘called’ with ‘considered’

Done

p. 25, line 6, Remove ‘yet’

Done

Reference

Steiner, N., 2001: Introduction of variable drag coefficients into sea ice models, Annals of Glaciology, 33, 181 – 186.

~~Probabilistic forecast using a Lagrangian~~ Impact of rheology on probabilistic forecasts of sea ice ~~model~~trajectories: application for search and rescue operations in the Arctic

Matthias Rabatel[1], Pierre Rampal[1], Alberto Carrassi[1], Laurent Bertino[1], and Christopher K. R. T. Jones[2]

[1]Nansen Environmental and Remote Sensing Center, Norway

[2]Department of Mathematics, University of North Carolina, USA

Correspondence to: Rabatel (matthias.rabatel@nersc.no or matthiasrabatel@gmail.com)

Abstract. We present a sensitivity analysis, and discuss the probabilistic forecast capabilities, of the novel sea ice model *neXtSIM* used in hindcast mode. The study pertains to the response of the model to the uncertainty on winds using probabilistic forecasts of ice trajectories. *neXtSIM* is a continuous Lagrangian numerical model, and uses an elasto-brittle rheology to simulate the ice response to external forces. The sensitivity analysis is based on a Monte Carlo sampling of 12 members. The response of the model to the uncertainties is evaluated in terms of simulated ice drift distances from their initial positions, and from the mean position of the ensemble, over the mid-term forecast horizon of ~~10-days~~10 days. The simulated ice drift is decomposed into advective and diffusive parts that are characterised separately both spatially and temporally and compared to what is obtained with a *free-drift* model, that is, when the ice rheology does not play any role on the modelled physics of the ice. The seasonal variability of the model sensitivity is presented, and shows the role of the ice compactness and rheology in the ice drift response at both local and regional scales in the Arctic. Indeed, the ice drift simulated by *neXtSIM* in summer is close to the one obtained with the ~~free-drift~~ *free-drift* model, while the more compact and solid ice pack shows a significantly different mechanical and drift behaviour in winter. For the winter period analysed in this study, we also show that, in contrast to ~~of free-drift~~ the *free-drift* model, *neXtSIM* reproduces the sea ice Lagrangian diffusion regimes as found from observed trajectories. The forecast capability of *neXtSIM* is also evaluated using a large set of real ~~buoys'~~buoy's trajectories, and compared to the capability of the ~~free-drift~~ *free-drift* model. We found that *neXtSIM* performs significantly better in simulating sea ice drift, both in terms of forecast error and as a tool to assist search-and-rescue operations, although the sources of uncertainties assumed for the present experiment are not sufficient for a complete coverage of the observed IABP positions.

1 Introduction

Large changes in the Arctic sea ice have been observed in recent decades in terms of the ice thickness, extent and drift (e.g. Kwok, 2007; Stroeve et al., 2007; Rampal et al., 2011; Stroeve et al., 2012). These changes, and the underlying driving mechanisms, still need to be fully understood in spite of their being fundamental for building confidence in the forecasting capabilities of current prediction systems. The need for a reliable sea ice prediction platform is particularly felt in the modern context of growing economic opportunities with high societal and environmental impacts. For instance, the dramatic decline of sea ice cover in the Arctic is opening new shipping routes, fishing grounds and tourist destinations as well as access to a significant portion of the remaining hydrocarbon resources. Associated with this increasing activity are important risks for pollution of the Arctic environment, and risk to human lives. High quality predictions of ocean and sea ice in the polar regions are therefore needed in order to measure the risks, to plan future activities, and to assist operations in real time.

Current short-term (i.e. within 10 days) sea ice forecasting systems integrate either a stand-alone sea ice model (~~RIPS (Lemieux et al., 2016)~~RIOPS (Lemieux et al., 2016; Dupont et al., 2015)), a coupled ice-ocean model (such as, e.g. ACNFS (Hebert et al., 2015), TOPAZ (Sakov et al., 2012) or GIOPS (Smith et al., 2015)), or more seldom a coupled atmosphere-ice-ocean model (GloSea5 (Williams et al., 2015)). Seasonal to decadal climate forecasts are more common and include sea ice as part of the Earth System Models (see, e.g. Carrassi et al. (2016)). The sea ice models used in these systems are usually derived from the work of Hibler III (1979), and they treat the sea ice as a continuous medium with a viscous-plastic rheology (Hunke and Dukowicz, 1997; Bouillon et al., 2009). In spite of this development, simple free-drift ice (i.e. in the absence of friction and internal forces) forecasts have remained in use by environment agencies (Grumbine, 1998, 2003). The forecast skill of these systems based on a free-drift ice has been evaluated in deterministic mode, when a single "best" forecast is provided: despite the lack of realism in the free-drift assumption, the forecast skill of such systems is seen as difficult to beat (Schweiger and Zhang, 2015).

Probabilistic forecasts, widely used in weather forecasting (Molteni et al., 1996; Leutbecher and Palmer, 2008), are still in their infancy in sea ice forecasting. Probabilistic predictions rely on an ensemble of model simulations (i.e. a Monte Carlo simulation) used to describe the forecast uncertainty stemming from errors in the model parameters, initial and boundary conditions as well as from any external forcing. The resulting cloud of model outputs is used to retrieve statistical information, such as the ensemble mean and its spread (i.e. the standard deviation), that are thus used in place of the deterministic forecast and to estimate the associated uncertainty, respectively. The multiple simultaneous sources of errors make the forecast accuracy of the ensemble mean usually exceed that of the single deterministic prediction (Leith, 1974; Zhu, 2005), although often the spread underestimates the actual forecast error when the sources of error are not all adequately accounted for (Buizza et al., 2005). Monte Carlo techniques are already common practice in different areas (e.g. Dobney et al., 2000; Hackett et al., 2006; Breivik and Allen, 2008; Melsom et al., 2012; Motra et al., 2016; Duraisamy and Iaccarino, 2017), and a common tool for sensitivity analysis.

This study concerns the probabilistic forecast capability of the sea ice model *neXtSIM* (Rampal et al., 2016b). The work is carried out by performing a Monte Carlo sensitivity analysis of the model with respect to uncertainties in the surface wind velocity. The first goal is to highlight the role of the ice rheology on the ice drift: how do the ensemble mean drift and its standard deviation respond to uncertainties in the wind forcing? To answer this question, we compare the ice drift obtained from *neXtSIM* to one obtained from a *free-drift* model. In the second part, we study the skill of the probabilistic forecast using Lagrangian trajectories departing from independent ~~in situ~~ virtual drifting buoys, and compare them with real observations ~~.~~

~~Without~~ without aiming to make it a key objective. We use the conceptual framework of search and rescue operations where a probabilistic forecast is commonly used to draw the search area of the ocean where drifting objects are likely to be found (Hackett et al., 2006; Breivik and Allen, 2008; Melsom et al., 2012). Contrary to these studies, the present simulations are in the context of a "hindcast-forecast", using reanalysed atmospheric forcing fields but assuming that they are affected by errors with the statistical properties that could be expected from a numerical weather forecast in the Arctic. For simplicity, we will use the word "forecast" instead of "hindcast-forecast" throughout the paper.

Our main research tool and object of study is the ~~advanced~~ sea ice model *neXtSIM*. The model *neXtSIM* is based on a Lagrangian numerical scheme and on a continuous approach using a newly developed elasto-brittle ice rheology. This mechanical framework is inspired by the scaling properties of sea ice dynamics revealed by multi-scale statistical analyses of observed sea ice drift and deformation (Marsan et al. (2004), Rampal et al. (2008) and Bouillon and Rampal (2015b)), as well as by the in situ ~~measures~~ measurements of sea ice internal stresses showing that sea ice deformation is accommodated by Coulombic faulting (Weiss et al. (2007), Weiss and Schulson (2009)). For 40 years, a large variety of sea ice models have been developed. Some, like *neXtSIM*, treat the sea ice as a continuous medium, yet with different rheologies (e.g. ~~visco-plastic (Coon et al., 1974; Hibler III, 1979),~~ Coon et al. (1974) and Hibler III (1979) modelled sea ice as an elasto-plastic material, Hunke and Dukowicz (1997) as an elasto-visco-plastic ~~, (Hunke and Dukowicz, 1997), or~~ material, or Dansereau (2016) as an Maxwell-elasto-brittle ~~, (Dansereau, 2016)~~material), are suitable for high ice concentration ($> 80\%$) while others, that treat the ice as a discrete medium (Hopkins et al., 2004; Wilchinsky et al., 2010; Herman, 2011; Rabatel et al., 2015), are more suitable for low ice concentration ($< 80\%$) such as within the marginal ice zone.

We concentrate here on the impact of the error from the wind field alone. The reasons are twofold: first, the wind is the most influential external force affecting sea ice motion. About 70% of the variance of the sea ice motion in the central Arctic can be explained by the geostrophic winds (Thorndike and Colony, 1982). However, the sea ice response to winds strongly depends on its degree of damage; sea ice responds in a linear way only when it is fragmented into small floes, indeed, in this case, the internal forces are negligible and the inertial term is linearly related to the air and water drags, whereas this behaviour drastically changes when considering a large, continuous and undamaged solid plate. The second reason ~~stands on the fact that~~ is due to surface wind velocity fields provided by atmospheric re-analyses contain large uncertainties in the Arctic due to the limited number of observations.

Previous sensitivity analyses of the *neXtSIM* model have been performed with respect to initial conditions and to some key sea ice mechanical parameters (see Sect. 4 in Bouillon and Rampal (2015a)). These analyses consisted in running the model with different values of the input sources. This allowed the authors to explore and quantify the sensitivity of the ice velocity with respect to the ratio between water and air drag coefficients, and of the ice deformation with respect to the compactness parameter value (see Eq. (5)), the sea ice cohesion value (see Eq. (10) in Bouillon and Rampal (2015a)), the initial concentration field, or the initial thickness field. Although these analyses did not use the ~~full complexity of the present version of~~ latest model

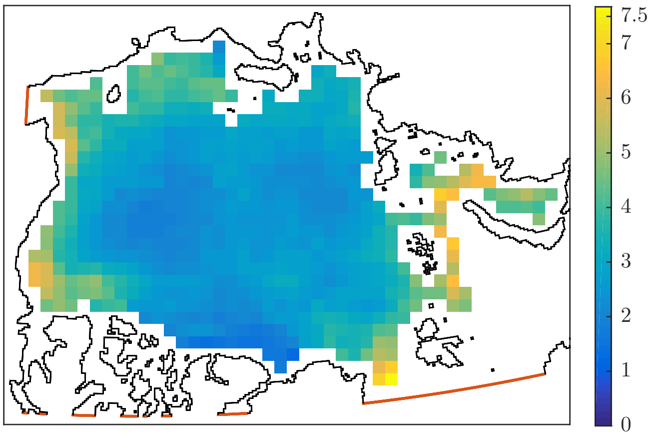

Figure 1. Systematic errors in the neXtSIM ice velocities, compared to observations from the OSI-SAF dataset. Simulated and observed ice drift are averaged over the period from 1 January 2008 to 30 April 2008. The cells with less than 28 observations over the winter are masked. The colour scale represents the velocity in $km\ day^{-1}$.

developments of *neXtSIM* (in particular they did not include the thermodynamics, nor the re-meshing process), the impact of ~~some~~ the mechanical parameters on the ice deformation can still be considered as valid.

Systematic errors in the mean sea ice drift are evaluatd by averaging modelled and observed drift from the OSI-SAF dataset (Lavergne and Eastwood, 2015) over the period between 1 January 2008 and 30 April 2008 and over boxes of $100 \times 100\ km^2$ covering the whole Arctic (see Fig. 1). The largest differences between the observed and simulated mean ice drift are located in the Beaufort, Chukchi, Kara and Barents Seas and Fram Strait and in some areas of the East Siberian sea. In the rest of the domain the error on the mean winter drift is only less than 3 $km\ day^{-1}$, consistently with Rampal et al. (2016b).

This paper is organized as ~~follow~~follows: Sect. 2 gives a general presentation of the sea ice model *neXtSIM* with the main equations describing the sea ice dynamical behaviour; Sect. 3 presents the details of the sensitivity analysis based on a Monte Carlo sampling, including the description of the quantities of interest, the construction of the wind perturbations, and the general experimental setup. In the same Sect. 3, we also define the *free-drift* model that will be used for comparison and benchmark against *neXtSIM*. Section 4 discusses the results for the ensemble mean, spread and the evaluation of the forecast skills comparing *neXtSIM* to the *free-drift* model. Final ~~conclusion~~ conclusions are drawn in Sect. 5.

2 ~~Generalities~~ General information on the model *neXtSIM*

In this section, we provide a general description of *neXtSIM*. Deliberately, we choose to not go through all model equations here, but rather list those that are needed to get an overall understanding of how the model works, and that are relevant for the present study. For a more detailed description of the model see Bouillon and Rampal (2015a) and Rampal et al. (2016b).

neXtSIM is a continuous dynamic-thermodynamic sea ice model. It uses a pure Lagrangian advection scheme, meaning that the nodes of the model mesh are moving at each time step according to the simulated ice motion. The model mesh is therefore changing over time, it is not ~~spatial~~ spatially homogeneous, and it can locally become highly distorted, that is, when and where the ice motion field is showing strong spatial gradients. In this case, a local and conservative re-meshing procedure is applied in order to keep the numerical integrity of the model and the spatial resolution of the grid approximatively constant during the simulation. The equations are discretised on a triangular mesh and solved using the classical finite element method, with scalar and tensorial variables defined at the center of the mesh elements, and vectors defined at the vertices. The model is using a mechanical framework that has been developed recently (Girard et al. (2009) and Bouillon and Rampal (2015a)), and which is based on the Elasto-Brittle (EB) rheology. The brittle mechanical behaviour of the sea ice is simulated by calculating the local level of damage in each grid cell, a variable which is not considered in classical viscous-plastic sea ice models typically used in the sea ice modelling community. Sea ice thermodynamic, which is parametrised in *neXtSIM* as in the zero-layer model of Semtner (1976), controls the amount of ice formed or melted at each time step. When a volume of new (and therefore undamaged) ice is formed within a grid cell by thermodynamical ~~refreezing~~freezing, the mechanical strength of the total volume of ice covering that cell is partially restored, and the new damage value is computed as a volume-weighted mean. Note however that the damaging process is very fast (i.e. about few minutes) while the mechanical healing process is occurring over much slower time scales of about several weeks. The sea ice variables used in *neXtSIM* are the following: h and h_{s} are the effective sea ice and snow thickness respectively (ice and snow volumes per unit area); A is the sea ice concentration (bounded to 1); d is the sea ice damage ranging from 0 (undamaged ice) to 1 (fully damaged); $\boldsymbol{u}$ is the horizontal sea ice velocity vector; and $\boldsymbol{\sigma}$ is the ice internal stress tensor. The model has two ice thickness categories: ice and open water.

The evolution equations for h, h_{s} and A (here denoted ϕ) have the following generic form

$$\frac{D\phi}{Dt} = -\phi\nabla\cdot\boldsymbol{u} + S_{\phi}, \tag{1}$$

where $\frac{D\phi}{Dt}$ is the material derivative of ϕ, $\nabla\cdot\boldsymbol{u}$ the divergence of the horizontal velocity and S_{ϕ} a thermodynamical sink/source term. The evolution of sea ice velocity comes from the following sea ice momentum equation, integrated over the vertical,

$$m\frac{D\boldsymbol{u}}{Dt} = \nabla\cdot(\boldsymbol{\sigma}h) - \nabla P + \boldsymbol{\tau}_{\mathrm{a}} + \boldsymbol{\tau}_{\mathrm{w}} + \boldsymbol{\tau}_{\mathrm{b}} - mf\boldsymbol{k}\cancel{\wedge}\times\boldsymbol{u} - mg\nabla\eta, \tag{2}$$

where m is the inertial mass, P is a pressure term, $\boldsymbol{\tau}_{\mathrm{a}}$ is the surface wind (air) stress, $\boldsymbol{\tau}_{\mathrm{w}}$ is the ocean (water) stress and $\boldsymbol{\tau}_{\mathrm{b}}$ is the basal stress in case of grounded ice parametrised as in Lemieux et al. (2015). The last terms are the Coriolis parameter, f, the upward pointing unit vector, $\boldsymbol{k}$, the gravity acceleration, $\boldsymbol{g}$, and the ocean surface elevation, η. The internal stress $\boldsymbol{\sigma}$ is computed as in Bouillon and Rampal (2015a) and Rampal et al. (2016b). Its evolution equation can be written as

$$\frac{D\boldsymbol{\sigma}}{Dt} = \frac{\Delta d}{Dt}\frac{\partial\boldsymbol{C}}{\partial d} : \boldsymbol{\epsilon} + \boldsymbol{C}(A,d) : \dot{\boldsymbol{\epsilon}}, \tag{3}$$

where d is the damage and $\dot{\boldsymbol{\epsilon}}$ is the deformation rate tensor defined as $\dot{\boldsymbol{\epsilon}} = \frac{1}{2}\left(\nabla \boldsymbol{u} + (\nabla \boldsymbol{u})^{\mathrm{T}}\right)$. $\boldsymbol{C}$ can be written as

$$\boldsymbol{C} = \frac{E(A,d)}{(1-\nu^2)} \begin{bmatrix} 1 & \nu & 0 \\ \nu & 1 & 0 \\ 0 & 0 & \frac{1-\nu}{2} \end{bmatrix} \tag{4}$$

with ν being the Poisson's ratio while $E(A,d)$ the effective elastic stiffness of the ice which depends on the ice concentration A and the damage d according to

$$E = Y e^{-\alpha(1-A)}(1-d) \tag{5}$$

where Y is the sea ice elastic modulus (Young's modulus) and α is the so-called compactness parameter.

The evolution equation for the damage is written as:

$$\frac{Dd}{Dt} = \frac{\Delta d}{\Delta t} + S_d, \tag{6}$$

where Δd is a damage source term calculated as in Rampal et al. (2016b) (Eq. (8)), and S_d is thermodynamical sink term which depends on the volume of new and undamaged ice formed over one time step as well as on time (See Rampal et al. (2016b), Sect. 2.3 for more details).

The air and oceanic drags, respectively $\boldsymbol{\tau}_{\mathrm{a}}$ and $\boldsymbol{\tau}_{\mathrm{w}}$ in Eq. (2), are written as a force per unit area in the quadratic form using the associated turning angle (Leppäranta, 2011)

$$\begin{aligned} \boldsymbol{\tau}_{\mathrm{a}} &= \rho_a C_a \left\|\boldsymbol{u}_{\mathrm{a}} - \boldsymbol{u}\right\| R_{\theta_a} \left(\boldsymbol{u}_{\mathrm{a}} - \boldsymbol{u}\right) \\ \boldsymbol{\tau}_{\mathrm{w}} &= \rho_w C_w \left\|\boldsymbol{u}_{\mathrm{w}} - \boldsymbol{u}\right\| R_{\theta_w} \left(\boldsymbol{u}_{\mathrm{w}} - \boldsymbol{u}\right) \end{aligned} \tag{7}$$

where $\|.\|$, R_{θ_a}, R_{θ_w}, $\boldsymbol{u}_{\mathrm{a}}$, $\boldsymbol{u}_{\mathrm{w}}$, ρ_a, ρ_w, C_a and C_w are, respectively, the Euclidean norm in $\mathbb{R}^2$, the rotation matrix through the angle θ_a and θ_w, the wind velocity, the ocean current, the air density, the water density, the air drag coefficient and the water drag coefficient. The values of the model parameters that are used for the simulations presented in this paper are listed in Table 1.

3 Sensitivity analysis

~~The sensitivity, or uncertainty analysis, are performed in order to understand and to quantify the relative importance of different input sources in the outputs. More specifically, we explore the output space of the model and, after the definition of a region of interest for this output space, we identify which model inputs and which values and uncertainties of the inputs better explain the model results in the chosen region. This type of analysis is an usual important previous step to determine optimal sampling strategies for both probabilistic forecast and ensemble-based data assimilation methods (e.g. Evensen, 2009).~~

3.1 Methodology

In this study, we perform a sensitivity analysis using a statistical approach based on Monte Carlo sampling of the model inputs. We focus on the response of the model to the uncertainties in the wind velocity field. In particular, we are looking at the

Table 1. Parameters used in the model with their values for the simulations performed for this study.

Symbol	Meaning	Value	Unit
ρ_a	air density	1.3	$\mathrm{kg\,m^{-3}}$
c_a	air drag coefficient	5.1×10^{-3}	–
c_a	air drag coefficient (for FD)	3.2×10^{-3}	–
θ_a	air turning angle	0	°
ρ_w	water density	1025	$\mathrm{kg\,m^{-3}}$
c_w	water drag coefficient	5.5×10^{-3}	–
θ_w	water turning angle	25	°
ρ_i	ice density	917	$\mathrm{kg\,m^{-3}}$
ρ_s	snow density	330	$\mathrm{kg\,m^{-3}}$
ν	Poisson coefficient	0.3	–
μ	internal friction coefficient	0.7	–
Y	elastic modulus	9	GPa
Δx	mean resolution of the mesh	10	km
Δt	time step	200	s
T_d	damage relaxation time	28	days
c	cohesion parameter	8	kPa
α	compactness parameter	-20	–

response of sea ice drift to wind perturbations representing these uncertainties. Our methodology is based on simulating Lagrangian trajectories of virtual buoys using an ensemble run of the *neXtSIM* model forced by slightly different (i.e. perturbed) wind forcing (see Sect. 3.2 for more details on the generation of the perturbed winds).

The velocity of a given virtual buoy is calculated on-line, at each time step, as a linear interpolation of the velocities simulated at the nodes of the mesh element containing that buoy (see Lagrangian approach in Sect. 2). Each virtual buoy is associated with ~~a~~ an initial position $\boldsymbol{x}_0 \in D$, with D being the initial domain, and a start date $t_0 \in Y$ where Y is the time period of interest of this study (see Sect. 3.2 for more details). A buoy trajectory is denoted $\boldsymbol{g}(\boldsymbol{x}_0, t_0, t)$ with $t \in [t_0, T]$, and where T defines the duration of the individual simulations. For each initial position $\boldsymbol{x}_0$ and start date t_0, we simulate N trajectories $\{\boldsymbol{g}_i\}_{i\in\{1,\dots,N\}}$ from N model runs, each one corresponding to a different realisation of the wind forcing. If a buoy ends up in an ice-free element, it is then untracked further and its trajectory discarded from the remaining analysis.

For each ensemble member (trajectory), we define the following Euclidean distances

$$
\forall i \in \{1,\ldots,N\}, \quad
\begin{aligned}
r_i(t) &= \|\boldsymbol{g}_i(\boldsymbol{x}_0,t_0,t)-\boldsymbol{x}_0\| \\
b_i(t) &= \|\boldsymbol{g}_i(\boldsymbol{x}_0,t_0,t)-\boldsymbol{B}(t)\|,
\end{aligned}
$$

where the quantity $r_i(t)$ is the distance of the member position at time t, $\boldsymbol{g}_i(\boldsymbol{x}_0,t_0,t)$, from its departure origin, $\boldsymbol{x}_0=\boldsymbol{g}_i(t=t_0)$. The second quantity, $b_i(t)$, represents the distance between the member position at time t and the ensemble mean position (i.e. the barycentre, $\boldsymbol{B}(t)$, of the ensemble), $\cancel{\boldsymbol{B}(t)=\sum_{i=1}^{N}\boldsymbol{g}_i(\boldsymbol{x}_0,t_0,t)}$$\boldsymbol{B}(t)=1/N\sum_{i=1}^{N}\boldsymbol{g}_i(\boldsymbol{x}_0,t_0,t)$, at the same time t (see the top panel of Fig. 2). We make use here of the convention of using boldface for vectors and matrices and normal face for scalar quantities; hereafter, we drop the explicit mention ~~on~~ of the dependence on $\boldsymbol{x}_0$ and t_0, to simplify the notation. Furthermore, we define a 2-dimensional time-dependent orthonormal basis, centred on $\boldsymbol{B}(t)$, and whose axes are the line connecting $\boldsymbol{x}_0$ to $\boldsymbol{B}(t)$, and its perpendicular. The components/coordinates of $\boldsymbol{g}_i(t)$ on this basis are hereafter denoted as $b_{i,\parallel}(t)$ and $b_{i,\perp}(t)$, as illustrated in the bottom panel of Fig. 2; they provide ~~informations~~ information on the spatial and temporal evolution of the ensemble spread and shape, and can also be used to look at how the virtual buoy positions are distributed around the ensemble mean over time.

With the individual r_i and b_i in hands, we compute basic, second-order, statistics. Let us consider their means, μ_r and μ_b,

$$
\mu_r(t)=\frac{1}{N}\sum_{i=1}^{N} r_i(t), \qquad \mu_b(t)=\frac{1}{N}\sum_{i=1}^{N} b_i(t), \tag{8}
$$

and the standard deviations, $\sigma_{b_\parallel}$ and $\sigma_{b_\perp}$, of the components $b_\parallel$ and $b_\perp$,

$$
\sigma_{b_\parallel}(t)=\sqrt{\frac{1}{N-1}\sum_{i=1}^{N}\left|b_{i,\parallel}(t)\right|^2} \quad \text{and} \quad \sigma_{b_\perp}(t)=\sqrt{\frac{1}{N-1}\sum_{i=1}^{N}\left|b_{i,\perp}(t)\right|^2}, \tag{9}
$$

as our main quantities of interest in the analysis that follows. ~~In particular, we use the standard deviations~~ We note that the mean of $b_{i,\parallel}$ and $b_{i,\perp}$ are zero (being barycentric coordinates) and do not appear in the calculation of standard deviations. Throughout the rest of this paper, $\sigma_{b_\parallel}(t)$ and $\sigma_{b_\perp}(t)$ are only used to compute the ratio

$$
R(t)=\sigma_{b_\parallel}(t)/\sigma_{b_\perp}(t), \tag{10}
$$

that provides a measure of the anisotropy of the ensemble spread of the virtual buoys positions around the barycentre $\boldsymbol{B}$ of the ensemble.

It is finally worth observing that the two quantities, r and b, provide complementary ~~informations~~information: the former about the advective component of the motion, whereas the latter on its diffusive part. The ensemble mean distance from the starting point, μ_r is a statistical estimate of the distance travelled by an ice parcel according to the ice advection properties of the motion field, while μ_b is the (mean) spread relative to the aforementioned distance and accounts for the diffusion properties of the motion; see the top panel of Fig. 2.

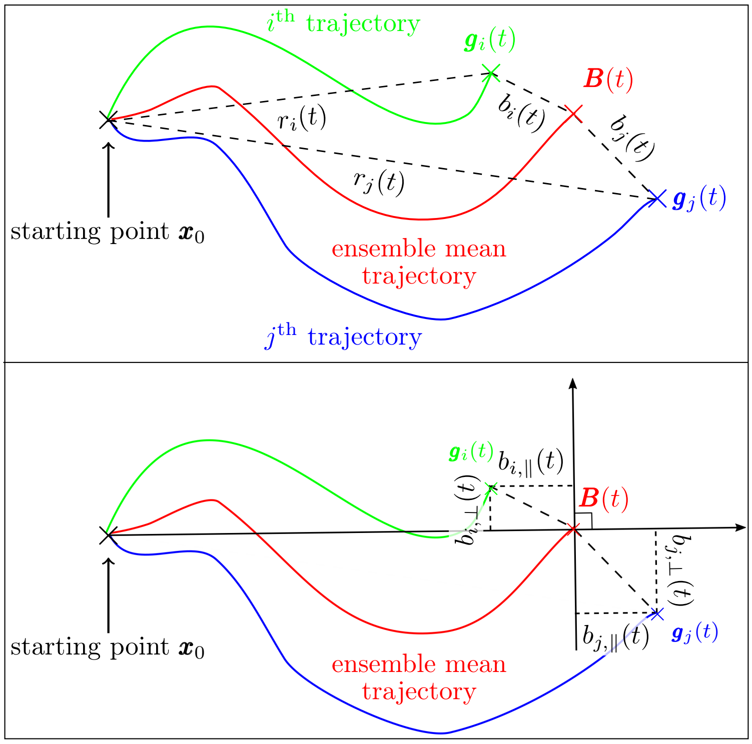

Figure 2. From a 12 ~~bouquet~~ member ensemble of simulated trajectories of a virtual buoy drifting during 10 days of which only two of them, denoted i and j, are drawn, we represent the distances r, b (top) and the coordinates $b_\parallel$, $b_\perp$ (bottom) for the virtual buoy i and j at time t.

3.2 Experimental setup

Our domain of study is the region covering the Arctic Ocean. While the coasts are considered as closed boundaries, open boundaries are set at the Fram and Bering Straits (see Fig 3).

The wind forcing is taken from the Arctic System Reanalysis (ASR) (Bromwich et al., 2012). This reanalysis product provides wind speeds and ~~direction~~ directions at 10 meters, every 3 hours~~and~~, at a horizontal resolution of 30 km. No turning angle has been applied (see Table 1). For every 3-hourly wind field, we generate spatio-temporal correlated perturbations as described in Evensen (2003), and then add them to the ~~basic wind fieldfrom the ASR~~ASR wind field. This procedure is identical to the one used to produce ensemble runs with the coupled ocean–sea ice model TOPAZ ~~(Sakov et al., 2012; Melsom et al., 2012). The main advantage of the method is~~ (Melsom et al., 2012) and constitutes the propagation step in the Ensemble Kalman Filter (Sakov et al., 2012). The method is designed such that the perturbed wind fields are keeping important physical properties, that is, the wind perturbations are geostrophic (gradients of random perturbations of the sea level pressure) and the wind divergence is kept ~~almost~~ unchanged. They are built on random stationary Gaussian fields, with a Gaussian spatial covariance function,

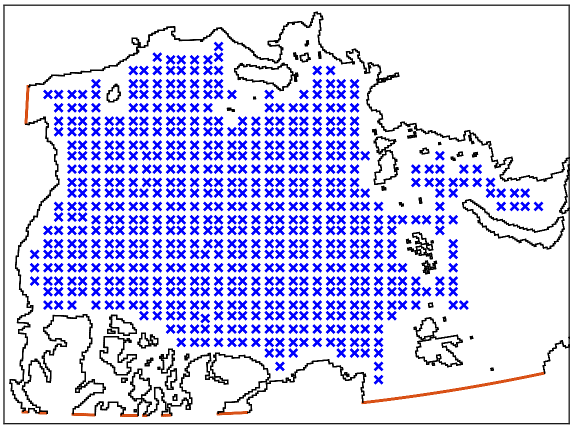

Figure 3. Maps showing the Arctic domain considered for this study. The red lines are open boundaries, while the black coastlines are closed boundaries. The starting points of the virtual trajectories simulated with the *neXtSIM* and FD models are represented by the blue crosses.

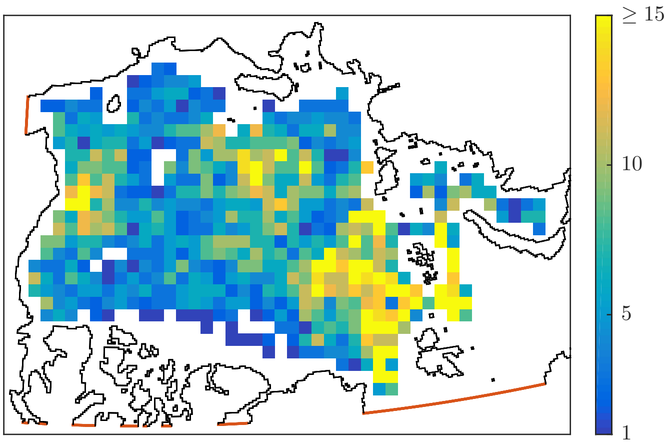

Figure 4. Spatial distribution of the number of occurrences of free drift events between 1 January 2008 and 30 April 2008. The temporal sampling frequency used is one day. These are the instances used for the optimisation of the air drag coefficient.

dimensionalised by the wind error variance and correlated in time. Time series of wind perturbations are assumed to be red noise. For our study, we used a decorrelation time-scale of 2 days, a horizontal decorrelation length scale of 250 km, ~~the~~ and the wind speed variance as equal to 1 $m^2\ s^{-2}$. These values are identical to those used in Sakov et al. (2012) except for a reduced wind speed variance ~~(6 times smaller).~~ to maintain a consistency with the ice rheology in *neXtSIM*. Indeed, a larger variance leads to an excess of ice breaking up beyond the physical behaviour expressed in *neXtSIM*.

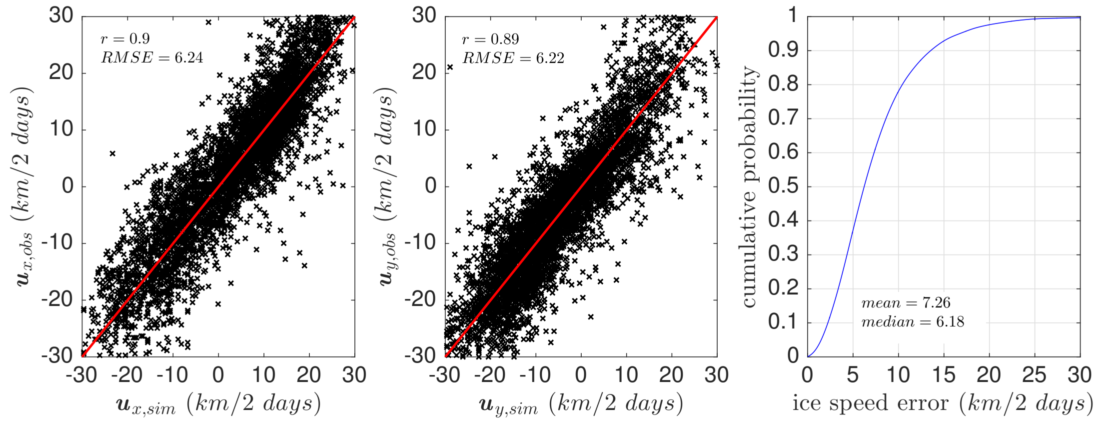

Figure 5. Scatter plots for the two components, x (left) and y (center), of the simulated (*neXtSIM*, x-axis) and observed drift (~~OSISAF~~ OSI-SAF dataset, y-axis) after the air drag optimisation procedure. The cumulative distribution of the ice velocity errors is shown in the rightmost panel.

Although the ensemble average of the ~~perturbations~~ perturbed u-, and v-components of the winds is equal by construction to the original ~~wind directions~~ winds provided by the ASR~~reanalysis~~, the wind speed is positively biased. The value of the air drag coefficient (C_a in Eq. (7)) had previously been optimised in the *neXtSIM* model when forced by the ASR ~~reanalysis following a method described~~ following the method presented in Rampal et al. (2016b), Sect. 3.2, and set to 7.6×10^{-3}. We applied the same method here to tune the value of C_a so that the simulated ice drift ~~compare~~ compares best with the observed ice drift from the ~~OSISAF~~ OSI-SAF dataset (Lavergne and Eastwood, 2015). The optimisation is carried out at all times between 1 January 2008 and 30 April 2008 but limited to the region where the ice is in ~~free-drift~~ free drift (see Fig. 4), that means, where the ensemble-average simulated ice velocity differs by less than 10% from the drift simulated by the free drift model (see the FD model below).

Figure 5 shows the comparison, after optimisation of the air drag coefficient, between the observed and simulated ice velocities. As expected for a wind dataset positively biased in magnitude compared to the original one, we found an ~~optimized~~ optimised value for the drag coefficient $C_a = 5.1 \times 10^{-3}$, lower than the one used in Rampal et al. (2016b) (7.6×10^{-3}).

The ocean forcing comes from the TOPAZ4 reanalysis (Sakov et al., 2012). TOPAZ4 is a coupled ocean-sea ice system combined with ~~a state-of-art~~ an ensemble Kalman filter data assimilation scheme assimilating both ocean and sea ice observations. In our simulations, we used the 30 m depth currents, to which we apply a turning angle of 25 degrees, the surface temperature and salinity, and the sea surface height, all provided as daily means with an average horizontal resolution of 12.5 km, following Rampal et al. (2016b).

Our analysis is based on two periods of the year 2008, respectively from 1 January to 10 May and from 1 July to 20 September, representative of the winter and summer conditions. We have intentionally studied them separately, because winter and summer are characterised by significantly different sea ice mechanical regimes, and therefore drift responses. During the winter, the whole Arctic basin is covered by ice and its concentration is close or equal to 100%, that is, the internal stresses in the ice, and the corresponding $\nabla \cdot (\boldsymbol{\sigma} h)$ term in Eq. (2), becomes ~~very large and dominant~~large and of the same order of magnitude as the wind drag term. As a consequence, the ice drift is (on average) much reduced. During the summer period, on the other hand, the ice concentration is lower and the ice pack does not generally reach the coasts, the ice internal stresses are ~~close~~ much closer or equal to zero, and the ice drift closer to a *free-drift* state (see text below). We ~~remark~~ note however that the wind field perturbations are generated using the same ~~procedure aforementioned~~ aforementioned procedure, for both the winter and the summer, and have thus the same spatial and temporal properties.

We ran a total of 13 ~~,~~ simulations in the winter ~~,~~and 8 ~~,~~in the summer ~~, simulations for successive~~during successive, non-overlapping~~10-days long ,~~ , 10 days-long periods. Limiting the length of the simulations to 10 days ensures that the ~~thermodynamical effect (increase in sea ice concentration or thickness) on the drift can reasonably be considered negligible along the track~~sea ice state (thickness and concentration) remains as realistic as possible in the free-drift simulation, in which there are no physical limits to the amount of ridging and opening. The starting positions are ~~spaced~~ separated by 100 km and cover the domain ~~as~~ displayed in Fig. 3. All ensemble members start from the same initial conditions extracted from a previous — deterministic — *neXtSIM* simulation by Rampal et al. (2016b) run without any perturbations of the winds. This concerns all sea ice variables : h, h_s, A, d, $\boldsymbol{u}$, $\boldsymbol{\sigma}$. We ran an ensemble of 12 members, each of them forced by the perturbed wind ~~dataset~~ generated as explained above. We performed (not shown) a convergence analysis of our results as a function of the ensemble size from $N = 3$ to $N = 20$, and observed a convergence from about $N = 10$ with only minor changes for $N \geq 12$, and are thus confident that $N = 12$ suffices to our purposes. From these ensemble runs we simulated a total of ~~8000~~ over 96 000 ($\simeq 8000 \times 12$) virtual buoy trajectories over the winter season, and ~~around 3200~~ over 38 000 ($\simeq 3200 \times 12$) trajectories over the summer season. This dataset was used to run the analyses described in Sect. 4 and presented at the 19th EGU General Assembly (Rabatel et al., 2017).

~~Maps showing the Arctic domain considered for this study. The red lines are open boundaries, while the black coastlines are closed boundaries. The starting points of the ensemble trajectories simulated with the *neXtSIM* and FD models are represented by the blue crosses.~~

As already stated, we compared *neXtSIM* with the so-called *free-drift* model, hereafter referred to as FD, so that all simulations that follow have been carried out for the two models. *neXtSIM*, Eq. (2) with all terms in its right-hand-side included, is our reference model. The FD model is equivalent to *neXtSIM* except that it considers the following simplified version of the momentum equation in which the terms related to the sea ice rheology, the basal stress and the inertial term are neglected

$$0 = \boldsymbol{\tau}_{\mathrm{a}} + \boldsymbol{\tau}_{\mathrm{w}} - mf\boldsymbol{k}\cancel{\triangle}\times\boldsymbol{u} - mg\nabla\eta. \qquad (11)$$

In Eq. (11) the water and air drag forces, the Coriolis force and the gravity force due to the ocean surface tilt are balancing each other. The FD model ~~therefore mimics the drift of a buoy~~ is therefore analogous to the steady state drift of an object at the surface~~of the ocean~~. We run the FD model with the same initial conditions as *neXtSIM* except that d and $\boldsymbol{\sigma}$ are not used. The drag coefficient is also optimised for the FD model at a value of 3.2×10^{-3}, which is lower than for *neXtSIM*, as expected. The optimisation method used for FD is the same as for *neXtSIM* described above, except that the OSI-SAF drift vectors are used everywhere.

4 Results

In this section, the notations $< . >_W$ and $< . >_S$ correspond to winter and summer averages (i.e. over all the 13 and 8 simulation periods of 10 days) respectively. The notations $< . >_D$ correspond to the spatial mean over the domain. When considering both spatially and temporally averaged quantities, we use the notations $< . >_{W,D}$ or $< . >_{S,D}$.

4.1 Spatial patterns

Figures 6 and 8 show maps of mean drifting distance and spread (see the definitions of μ_b and μ_r in Sect. 3.1) of the virtual buoys after $t = 10$ days, averaged over the 13 (winter) and 8 (summer) successive simulations. Similar results are obtained for different time $t \in [0, 10]$ days (not shown). The pixels on the maps correspond to boxes of 100×100 ~~km~~ km^2 centred on the initial positions $\boldsymbol{x}_0$ where the virtual buoys have been deployed at t_0.

Figures 7 and 9 are the counterparts of Figs. 6 and 8 and show the average wind speed (left panel) and ice thickness (right panel) for winter (Fig. 7) and summer (Fig. 9) respectively. Note that both figures are relative to *neXtSIM*, but the free-drift wind speed is identical (same perturbations) and the ice thickness geographical pattern very similar; we have thus omitted to display them to avoid redundancy.

From Fig. 6 and 8 we see that *neXtSIM* gives a smoother response to perturbed forcing than the FD model in terms of mean advective drift μ_r and mean diffusive spread μ_b, in both winter and summer. Indeed, we observe in *neXtSIM* a clear spatial coherency in both the advection and diffusion of the ice buoys over the domain that is almost ~~completely~~ absent in FD~~for which the obtained fields appear almost random~~. We believe that this behaviour is related to the mean ice thickness pattern and, to a lesser extent, to the mean wind speed pattern (see Figs. 7 and 9 for winter and summer respectively).

For *neXtSIM*, the smallest values for the mean of μ_r and μ_b averaged over the winter time period are found in the area located north of Greenland and the Canadian Archipelago, which is where the ice is the oldest, thickest ($> 4\ m$) and mechanically the strongest, and where the winds are on average weaker as compared to the rest of the Arctic. On ~~another~~ the other hand, in the surrounding Seas (i.e. Beaufort, Bering, ~~Chucky~~Chukchi, Kara and Barents Seas from West to East), where the ice is thinner and the winds stronger, the mean of μ_r and μ_b are larger. Note that in summer these correlations or anti-correlations are even

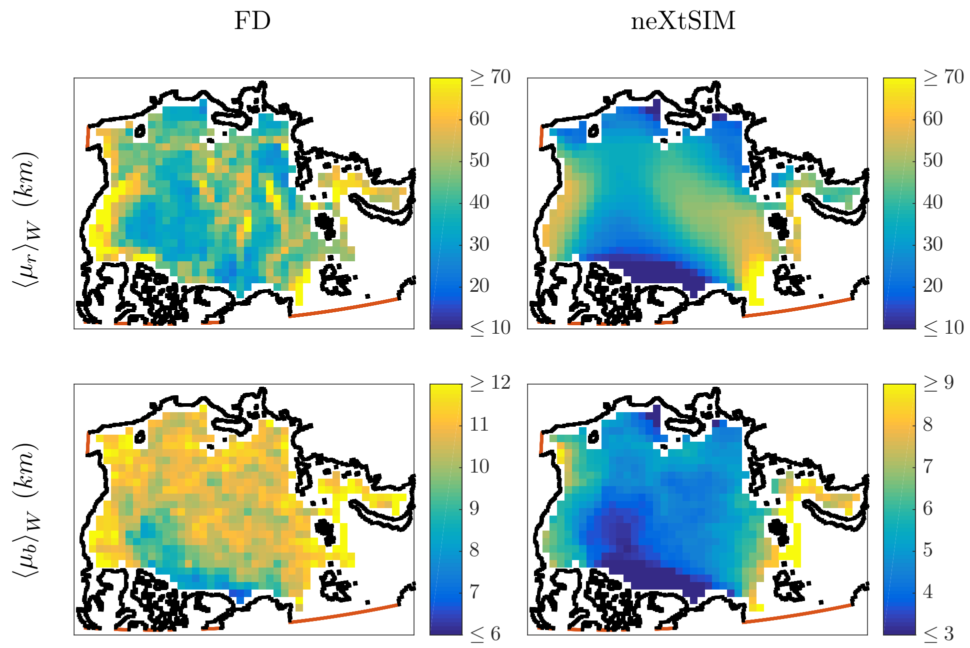

Figure 6. Mean over the winter period of $\mu_r(t)$ and $\mu_b(t)$ at $t = 10$ days. The calculated values are represented by coloured squares centred on the starting points $\boldsymbol{x}_0$ shown in Fig. 3.

stronger, for example between the means of μ_b and the ice thickness (see Figs. 8 and 9).

For FD, ~~and for both winter and summer,~~ the mean values of μ_r are ~~less~~ correlated to the ~~thickness field than in *neXtSIM*, but still strongly correlated to the wind speed~~ wind speed in winter and, to a lesser extent, in summer (left panels ~~inn~~ in Fig. 7 and 9)~~, whereas the spatial pattern of the mean of μ_b shows no coherence compared to *neXtSIM* and looks noisy~~. It is worth noting that, despite the presence of thick ice in the north of the Canadian Archipelago and low winds, the ice is still advected significantly, as opposed to what is obtained with *neXtSIM*. Moreover, the spatial pattern of the mean of μ_b shows no spatial coherence and resembles the random patterns from the wind perturbations. It is clearly visible in summer, while in winter the sea ice thickness field stays discernible. This may be due to the presence of the ice mass in Eq. 11.

In both winter and summer, the ~~response~~ time-average response of μ_r and μ_b to wind perturbations is overall lower ~~by 35%~~ in *neXtSIM* than in FD (except in summer when μ_r is 7% larger in *neXtSIM*). This can be attributed to the ~~fact that the ice rheology is taken into account~~ ice rheology being turned on in *neXtSIM*, thus acting as an additional filter on the momentum transferred from the wind to the ice. In more details, it is interesting to note that the magnitude of the impact of the ice rheology is different whether we ~~look at the drifted~~ consider the drift distance by advection r or the spread distance by diffusion b and ~~during~~ consider the winter or the summer. ~~Averaged~~ On average over the winter, $\langle \mu_r(t) \rangle_D$ and $\langle \mu_b(t) \rangle_D$ are respectively

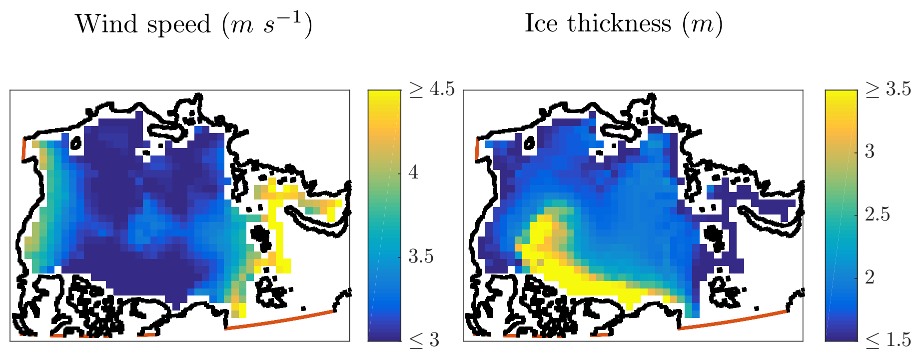

Figure 7. Winter average of wind speed and ice thickness. Both maps are from the *neXtSIM* simulations, but similar thickness field and exact same wind speed field are obtained for the FD simulations.

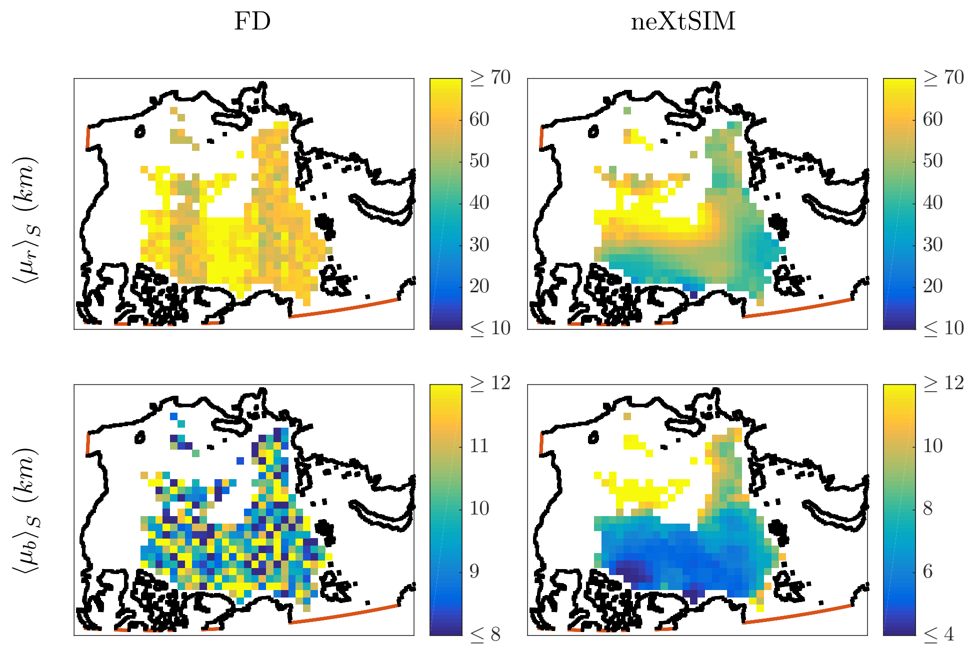

Figure 8. Mean over the summer period of $\mu_r(t)$ and $\mu_b(t)$ at $t = 10$ days. The calculated values are represented by coloured squares centred on the summer starting points $\boldsymbol{x}_0$ (not shown).

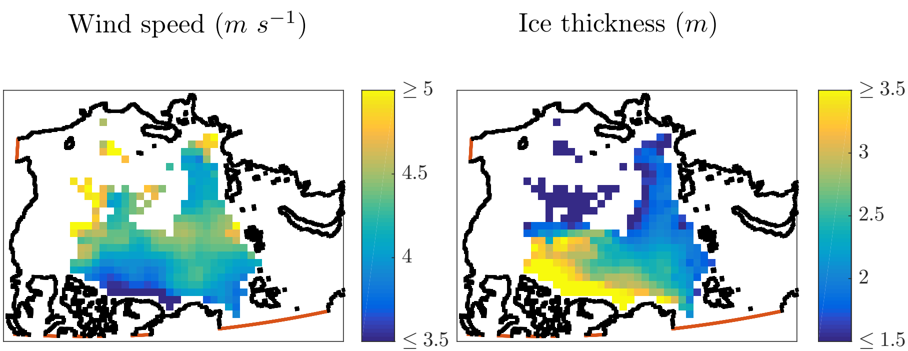

Figure 9. Summer average of wind speed and ice thickness. Both maps are from the *neXtSIM* simulations, but similar thickness field and exact same wind speed field are obtained for the FD simulations.

~~35% and 63~~21% and 52% lower in *neXtSIM* than in FD at $t = 10$ days, whereas over the summer, ~~$\langle \mu_r(t) \rangle_D$ and~~ $\langle \mu_b(t) \rangle_D$ ~~are respectively 14% and 39%~~ is 21% lower. This large difference between the two distances, especially in winter, is probably related to the high ice concentration making sea ice harder to break up, and keeps the members closer to each other. During summer, the ice is generally much less packed and the physical/dynamical differences between *neXtSIM* and FD have a lower impact. The 7% larger values of μ_r for *neXtSIM* are likely related to the optimisation of the air drag coefficient that returned a larger coefficient for *neXtSIM*.

As expected, for *neXtSIM*, we observe an increase of $\mu_r(t)$, of about 51%, and $\mu_b(t)$, of about 69%, in summer compared to winter. This behaviour differs drastically from the FD for which the values are nearly the same for both periods, and it is presumably related to the decrease in ice concentration due to the summer melting. The averaged sea ice concentration over the whole domain in winter is about 0.99 while it drops to 0.83 in the summer. In *neXtSIM*, this strongly ~~influence~~ influences the mechanical behaviour of the sea ice since the effective elastic stiffness E depends non linearly on the ice concentration (see Eq. (5)). Assuming no change in the average level of damage of the ice, a drop by 15% of the ice concentration between winter and summer implies a reduction of E by 96%. This reduction of E leads in turn to a significant decrease of the internal stresses within the ice, thus lowering the term $\nabla \cdot (\boldsymbol{\sigma} h)$ in Eq. (2), which makes the ~~buoy's~~ buoys drift in *neXtSIM* closer to the ~~one~~ ones obtained with the FD model.

The absolute values of μ_r and μ_b obtained by our analysis reveal that the advection part of the motion is in general larger than the diffusive part, independently of the season under consideration. In FD the ratio $\gamma = \mu_r(t)/\mu_b(t)$ at $t = 10$ days is about ~~4.~~ 4.5. In *neXtSIM* though, the ice rheology is acting in increasing this ratio to 7. However, this value presents a strong spatial variability depending on the local thickness and wind speed. Where both are large, γ is large. For example, such areas are observed in the Fram Strait in winter ($\gamma > 10$), and in the central Arctic in summer ($\gamma > 12$). Where both ice thickness and

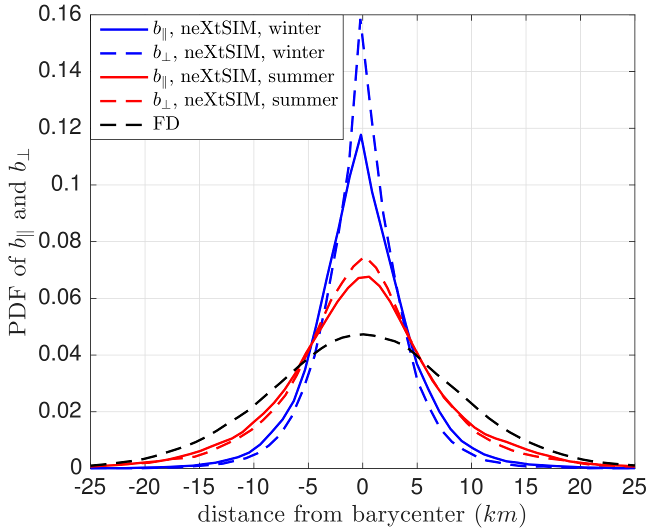

Figure 10. Probability density function of $b_{\|}(t)$ (solid lines) and $b_{\perp}(t)$ (dotted lines) at $t = 10$ days for *neXtSIM* in the winter (blue) and summer (red). The PDFs from FD are similar for summer and winter, and for $b_{\|}(t)$ and $b_{\perp}(t)$, and are therefore shown as a single black dashed line.

wind speed are small, γ is small. For example, this is the case around the new Siberian islands in winter ($\gamma < 4$), and close to the ice pack edge in summer ($\gamma < 6$).

4.2 Spatial and temporal properties of the ensemble spread

Figure 10 shows the probability density function (PDF) of $b_{\|}(t)$ and $b_{\perp}(t)$ at t =10 days for both *neXtSIM* and FD, and for winter and summer (see Sect. 3.1). The PDFs of $b_{\|}$ and $b_{\perp}$ for the FD case are almost identical, thus we chose to only display one curve (black dashed line). The first aspect to remark from Fig. 10 is that all distributions are uni-modal and symmetric, suggesting that the 2D-shape of the ensemble is symmetric around its barycentre $\boldsymbol{B}$. However, we notice that the ensemble is anisotropic in *neXtSIM*, that is, the distributions of $b_{\|}$ and $b_{\perp}$ differ substantially, whereas it is close to isotropic in FD.

Figure 11 shows the temporal evolution over 10 days of the ~~Arctic-averaged~~ Arctic averaged ratio R, Eq. (10), that defines the degree of anisotropy of the ensemble spread (1: isotropic; $>$ 1: anisotropic). We observe on the one hand that R is very close to 1 and relatively constant over time in the FD model. On ~~another~~ the other hand, it is systematically larger in *neXtSIM*, especially in winter, and it also displays a certain short-term variability. Here again, we encounter the peculiar effect of the *neXtSIM* mechanical response to the external forces, which is to break up and deform along fractures that are dispersing the different members of the ensemble along a preferential direction; such a behaviour cannot be reproduced by the FD. Note also that R is as large as 2 within ~~day 1 and 2~~ the first two days for *neXtSIM* in the winter, and ~~it then monotonically decrease~~

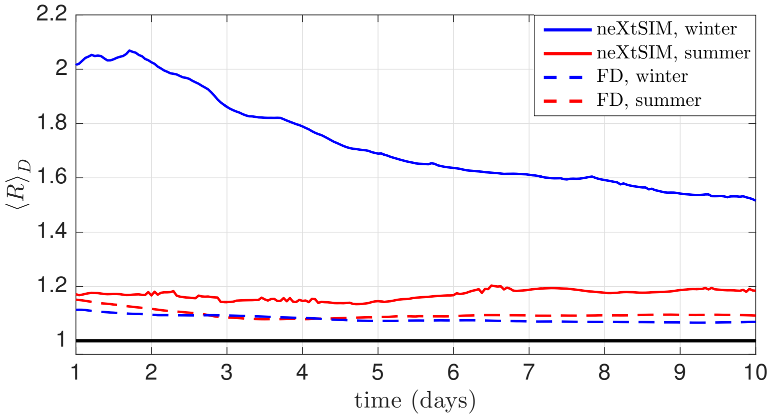

Figure 11. Evolution of the spatial mean of $R(t)$ from $t = 1$ to $t = 10$ days for the winter (blue) and summer (red) periods for *neXtSIM* (solid lines) and FD (dashed lines).

then it decreases monotonically for $t > 2$, ~~but it still remains~~ still remaining very large (between 1.4 and 1.6 at $t = 10$ days). This reveals that the ice will first tend to move compactly along the ~~wind direction~~ initial fractures (identical for all members at $t = 0$) away from the origin, but it then starts to break and~~depart~~, after 2 days, the damage pattern becomes significantly different within each members leading to a more isotropic ice dispersion away from the barycentre.

In Fig. 12, we show the maps of the $R(t)$ values computed for each ensemble of trajectories at $t = 10$ days. These values are represented as coloured squares centred on the starting point $\boldsymbol{x}_0$. We observe that highest degree of ensemble anisotropy ($R > 1$) is found north of Greenland and Canadian Archipelago, where the ice is the thickest and the ice drift and winds the lowest, in overall agreement with the interpretation of the temporal evolution of R for *neXtSIM* in the winter, provided in relation with Fig. 11. ~~Similarly, as~~ Globally, we observe a high (> 1.5) anisotropy close to the coasts, that can be explained by the ice pressure that counteracts sea-ice motions towards the coasts (and the associated dispersion as well). In summer, large stretches of the coasts are ice-free and the increase of R is less visible. This is in contrast to the pattern from FD. In absence of internal stresses, the pattern of the anisotropy exhibits no spatial coherence and is similar in both winter and summer periods. Furthermore, as already noticed from Fig. 11, the values obtained for *neXtSIM* are systematically larger (~~of~~ by about 65%) than for FD during the winter whereas only 8% larger during the summer. Yet, and remarkably, the values of R, and thus the anisotropy of the ice drift, for *neXtSIM* exhibit marked spatial correlations that are ~~almost absent in~~ absent from FD.

Another important characterisation of the ensemble spread evolution can be set by looking at the variance of the distance b between the virtual buoys and the barycentre $\boldsymbol{B}$ over time. The goal is to identify the diffusion characteristics of the ensemble, which can be interpreted in the framework of the turbulent diffusion theory of Taylor (1921). Similar Lagrangian diffusion analysis has been applied to study the regimes of diffusion of surface drifters in the ocean (e.g. Zhang et al., 2001; Poulain and

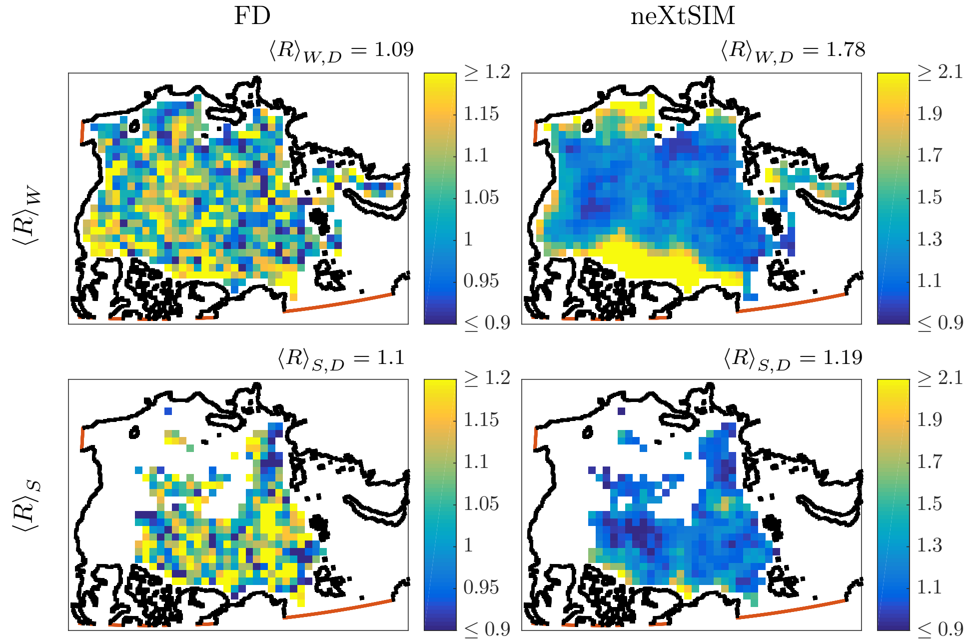

Figure 12. Means over the winter (top panels) and summer (bottom panels) of $R(t)$ at $t = 10$ days. The values are represented by coloured squares centred on the starting points $\boldsymbol{x}_0$. The spatio-temporal mean values (i.e. domain averaged and seasonally averaged) are calculated for each model and displayed above each panels for reference.

Niiler, 1989), and more recently of buoys fixed to the ice cover (e.g. Rampal et al., 2009; Lukovich et al., 2015; Gabrielski et al., 2015; Rampal et al., 2016a). In the analysis performed here, the distance b to the barycentre of the ensemble corresponds to the fluctuating part m' of the motion m in the so-called *Taylor's decomposition* $m = \overline{m} + m'$. Figure 13 shows the temporal evolution of the ensemble average of the distances b_i averaged over the Arctic domain D calculated form the buoy's tracks simulated with *neXtSIM* and FD. We found that the ensemble spread ~~follow~~ follows two distinct diffusion regimes, one for small time $t \ll \Gamma$ and one for large time $t \gg \Gamma$ where Γ is the so-called *integral time scale* (Taylor, 1921)~~, which is about 1.5 days for sea ice according to Rampal et al. (2009).~~ . In *neXtSIM*, the first regime we found for winter corresponds to the *ballistic* regime where $\left\langle \langle {b_i}^2 \rangle \right\rangle_D \sim t^2$, and the second to the *Brownian* regime where $\left\langle \langle {b_i}^2 \rangle \right\rangle_D \sim t$. These ~~two regimes are reproduced by *neXtSIM* in our winter simulations. These~~ results are in agreement with the wintertime sea ice diffusion regimes revealed by applying the Lagrangian diffusion analysis to the buoy trajectories dataset of the International Arctic Buoy Programme (Rigor, 2002) (Rampal et al., 2009) in wintertime, and shows that our experimental setup based on ensemble simulations forced by perturbed winds does not alter the capability of the *neXtSIM* model to reproduce ~~the propertiesof sea ice diffusion that was reported~~ these properties, as also shown recently in Rampal et al. (2016a) ~~. One should note that for FD, for both periods, and for~~ for the same winter. However, we note that the regime we obtain with *neXtSIM* ~~during the summer ,~~ for the summer 2008 is *super-diffusive*, with $\left\langle \langle {b_i}^2 \rangle \right\rangle_D \sim t^{1.15}$ for $t \gg \Gamma$~~meaning that~~ , and therefore in apparent contradiction with

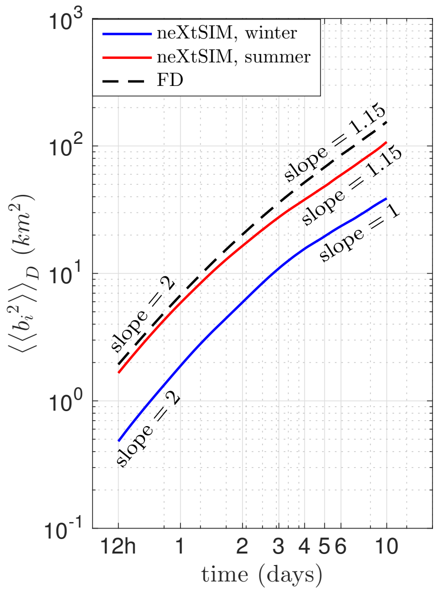

Figure 13. Spatial domain average of the variance of the distances b_i as a function of time from $t = 12$ hours to $t = 10$ days, for the *neXtSIM* (solid) and FD (dashed) models, and for winter (blue) and summer (red). The results for winter and summer being identical in FD, only one curve is plotted (black dashed line). The Brownian regime (slope $= 1$) is reached by *neXtSIM* during the winter, while in the other cases, a *super-diffusive* regime is obtained (slope $= 1.15$).

Rampal et al. (2009) who found that sea ice follows a same brownian regime in both winter and summer when averaging over the period 1979-2007. We suggest that this could rather be the fingerprint of a change in the dynamical behaviour of sea ice in summer that occurred over the most recent years (including 2008), in which the rheology is playing a weaker role than it was in the ~~simulated growth of the ensemble is~~ 80's and 90's. This is also supported by the results we obtain here with the FD model that neglects the rheology, and which exhibits *super-diffusive* ~~and in disagreement with the observations.~~ regime for 2008, regardless of the season considered.

4.3 Predictive skills of *neXtSIM* and of the FD models

We evaluate here how well the *neXtSIM* and FD models are able to forecast real trajectories in hindcast mode. As a benchmark, we compare the ensemble runs from ~~each model~~ both models to 604 (in winter) and 344 (in summer) observed trajectories from the IABP dataset. The simulated trajectories of both *neXtSIM* and FD are initiated on the same initial positions and at the same time as the IABP buoys, and are displayed in Fig. 14; the positions of IABP buoys are known every 12 hours. It is important to note that most of these buoys were deployed in regions of thick and compact ice, which drift is largely influenced by the sea ice rheology. Therefore, we expect the FD model to be less competitive than if the comparison data had been uniformly

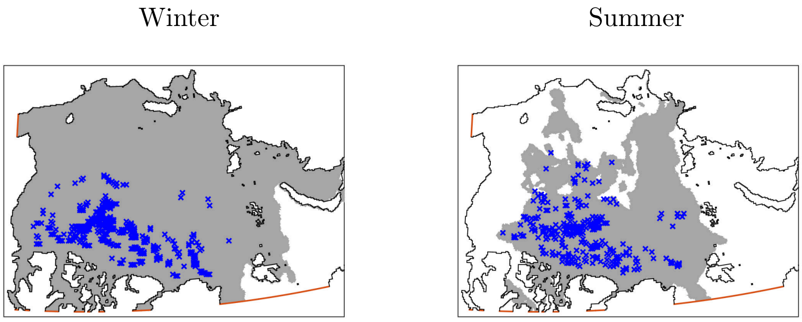

Figure 14. Maps showing the positions (blue crosses, 603 during winter and 344 during summer) of the IABP ~~buoy's~~ buoys trajectories dataset used in this study as starting point of the ensemble trajectory simulations performed with the *neXtSIM* and FD models. The grey area ~~is showing~~ marks the ~~mean~~ presence of the sea ice ~~coverage over~~ during at least 10 consecutive days (the ~~period considered for~~ length of the simulations) during the winter and summer periods.

distributed across the Arctic.

As a metric for the models skill inter-comparison, we use the linear *forecast error* vector

$$\boldsymbol{e}(t) = \boldsymbol{B}(t) - \boldsymbol{O}(t), \tag{12}$$

defined as the distance between the observed IABP buoy position, $\boldsymbol{O}(t)$, and that of the ensemble mean, $\boldsymbol{B}(t)$ (see also Fig. 16). The components of $\boldsymbol{e}(t)$ onto the orthonormal basis centred on $\boldsymbol{O}$ (see Sect. 3.1, Fig. 2 and 16), read $e_{\parallel}(t)$ and $e_{\perp}(t)$. We complete this evaluation comparing results from both models with those from a single deterministic forecast in order to verify the advantage of probabilistic forecasts. In this case, we run *neXtSIM* with parameters found in Rampal et al. (2016b), except the air drag coefficient has been re-tuned to $C_a = 6.5 \times 10^{-3}$ and unperturbed winds. For this new air drag coefficient, the same optimisation process as the probabilistic case is used against the same observations.

Figure 15 shows the average ~~module~~ norm of the forecast error, $\|\boldsymbol{e}\|$, and of its components, $e_{\parallel}(t)$ and $e_{\perp}(t)$, as a function of time, for the experiments with *neXtSIM* and FD, and for both winter and summer. Results reveal that the forecast error is smaller in *neXtSIM* than FD in both seasons. In winter, the error of the FD model grows almost twice as fast as the error of *neXtSIM*, up to ~~28.5~~ 26 km at day 10 compared to ~~14.6~~ about 15 km for *neXtSIM*.

~~Mean of the absolute forecast error $\|\boldsymbol{e}\|$ and vector components $e_{\parallel}$ and $e_{\perp}$ in the directions along and across the mean trajectory, as a function of drift duration. *neXtSIM* is represented by solid lines, while FD is shown as dashed lines. Winter is in blue and summer in red.~~

As already deduced from the results in the previous section, the mechanics underlying of the ice drift in *neXtSIM* and FD ~~get very~~ are similar in the summer, and this is reflected by the two errors being much closer to each other: the difference between

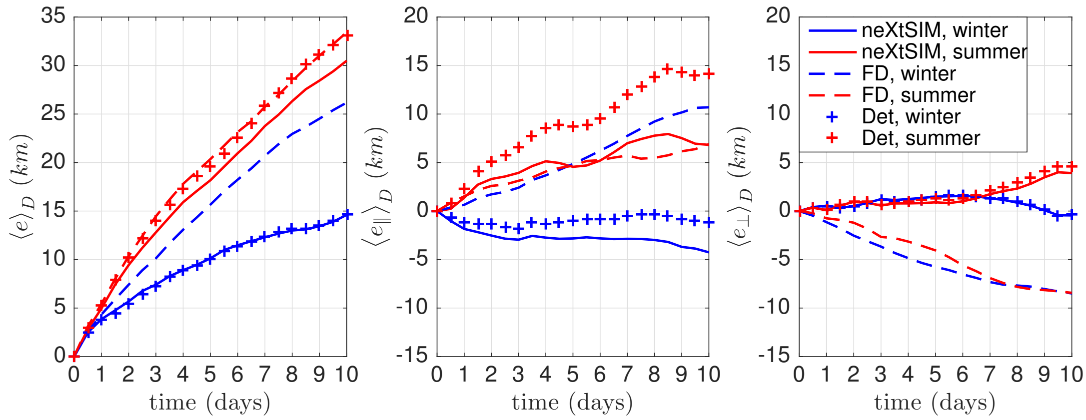

Figure 15. Mean of the absolute forecast error $\|\boldsymbol{e}\|$ and vector components $e_\parallel$ and $e_\perp$ in the directions along and across the mean trajectory, as a function of drift duration. *neXtSIM* is represented by solid lines, FD is shown as dashed lines, and the deterministic runs with cross marks. Winter is in blue and summer in red. A positive $e_\perp$ represents a drift to the left of the trajectory.

the two increases slower, reaching ~~$\simeq 4$~~ $\simeq 3$ km after ~~4~~ 10 days (see the left panel in Fig. 15).

The central panel in Fig. 15 shows a positive bias of the error in the along-drift component ($e_\parallel$) for both models and both periods, except for *neXtSIM* in winter which presents a negative bias. ~~Nevertheless, the biases in *neXtSIM* are all as small as one third of the corresponding ones in the FD model.~~ The general positive biases betray a too fast drift in the direction along the ensemble mean drift compared to the observations. Nevertheless, the bias for winter in *neXtSIM* is 2.5 times smaller than in the FD model, whereas both models perform similarly in the summer.

Finally, the right panel in Fig. 15 also reveals a bias of the error in the direction across the ensemble mean drift, yet substantially weaker than in the previous case. For FD, $e_\perp$ still being ~~positive~~ negative for both periods ~~,~~ corresponds to a drift too far to the right ~~in~~ compared to the observations. This bias ~~should be explained by the fact the Coriolis effect depends on the velocity, which is generally higher in the FD model; the larger the velocity the larger the Coriolis effect. With *neXtSIM*, these biases are much weaker in both periods. Overall, the performances are best for *neXtSIM*, especially in winter~~ to the right could be further reduced by a separate tuning of the turning angle θ_w for the FD and *neXtSIM* models. Overall, we conclude that the performances are significantly better for *neXtSIM* in winter, but similar in summer and this would likely remain so even after optimal tuning of the turning angle.

Comparing to a single deterministic *neXtSIM* forecast, we note that the forecast error is close to the average of the probabilistic run, although larger in summer reaching 34 km at 10 days. The main difference with the probabilistic run is the poorer along-drift component $e_\parallel$. Indeed, the error is closer to zero in winter and increases to 15 km in summer.

In Hackett et al. (2006); Breivik and Allen (2008), Monte Carlo techniques are used to forecast the drift of an object on the ocean surface. They associate the density of trajectories at their end points to a density of probability and use them to define a search area, within which the object is likely to be found. The search area is characterised by a surface centred on the ensemble mean and which size increases with the ensemble spread. The same methodology is followed here for forecasting the location of an object on drifting sea ice. In the context of rescue operations, the search area should be large enough to contain the actual position of the object, but not excessively large so as to keep the rescue operations time and resources affordable and efficient. The forecast system should therefore ideally yield a high probability to find the object in the search area, while keeping at the same time the search area as small as possible for the cost-efficiency of the rescue procedure.

The probability to find ~~the~~ a drifting object inside the search area, is referred to as the *probability of containment*, POC, and ~~reads~~

$$POC \propto \frac{Area}{\|\boldsymbol{e}\|^2}.$$

~~POC is proportional to~~ computed by counting the objects falling within the search area divided by the total number of objects. The POC may be interpreted as the ratio of the size of the search area to the square forecast error. ~~A small fore cast~~ Thus, a small forecast error compared to the search area leads to a strong POC; conversely, a small search area (ensemble spread) compared to the forecast error leads to a poor POC.

In order to evaluate the probabilistic forecast capabilities of *neXtSIM* and the more classical FD model, the context of a *search and rescue operation* is adopted. We assume that an IABP buoy has been lost for 10 days: its initial position, $\boldsymbol{x}_0$ (see Fig. 14), is assumed to be its last known position. The search area is then defined as the smallest ellipse centred on the ensemble mean position, $\boldsymbol{B}(t)$, encompassing all simulated ~~ensemble of buoys of~~ members of the ensemble at time t. The main axes of the ellipse, $a_{\|}$ and $a_{\perp}$, are aligned respectively with the parallel and perpendicular directions from the initial position, as defined in Sect. 3.2, and illustrated in Fig. 16. Similarly to Eq. (10) an anisotropy ratio $R = a_{\|}/a_{\perp}$ can be defined: R can be large due to the sea ice rheology. A search area defined in this way is increasing with the ensemble spread and contains 100% of the ensemble members.

Short of related literature for search and rescue in sea ice, we consider the values of open ocean search areas and POC found in Breivik and Allen (2008) and Melsom et al. (2012), as reference. These are respectively of the order of 1000 km^2 and 0.5, after 2 days of drift in the North Atlantic. We do not expect however a direct correspondence of these values to those of this section. First the sea ice is a solid, held together by the ice rheology, in particular in high concentration areas, so that the ensemble spread is expected to be smaller than in the open ocean. Second, the currents in the North Atlantic are generally stronger than in the Arctic Ocean. Finally, the search areas may be more complex than just an ellipse; it may well be a set of disjoint areas, each one with an associated different POC (e.g. Abi-Zeid and Frost, 2005; Breivik and Allen, 2008; Guitouni and Masri, 2014; Maio et al., 2016).

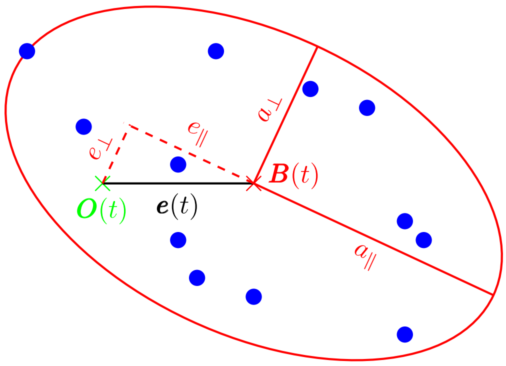

Figure 16. Illustration of the forecast error and the anisotropic search area. Blue dots represents the position of one member, while the barycentre of the ensemble (its mean) is $\boldsymbol{B}(t)$. The observation $\boldsymbol{O}(t)$ is in green and the forecast error is defined in Eq. (12). See text for definitions of the search ellipse and anisotropy ratio.

Figure 17 shows the evolution of the ellipse areas, averaged over all IABP buoys. The increase is nearly linear for both model configurations and seasons. After 2 days of drift in *neXtSIM*, the area does not exceed 100 km^2 in summer and not even half as much in winter. The area is larger in FD, and there is very little difference from winter to summer. The area for the FD is around ~~300~~ 200 km^2 after 2 days and it ~~almost reach 1000~~ reaches 500 km^2 after 5 days. The search area in FD is about ~~10~~ 7 times larger than in *neXtSIM* in the winter and ~~4~~ 2.5 times larger in the summer. Therefore, even if the forecast errors are smaller in *neXtSIM* than in FD, its shrunk search areas lead to a smaller POC for *neXtSIM* than for the FD model (not shown)~~: in practice the~~ .

On Fig. 18, we show the spread-error relationship for both periods and both models. The curves represent the spatial mean of the forecast error. Overall, the curves are above the black line, indicating that the forecast error is larger than the spread for both models. The probabilistic forecast from ~~*neXtSIM* is~~ both model during both period are therefore *too optimistic*~~, underestimates the uncertainties in the forecast, while the FD forecast overestimates them~~: they underestimate the uncertainties of their forecast. However, it is interesting to note two properties of *neXtSIM*. First, for spreads larger than 4 km, the forecast error from *neXtSIM* becomes independent from the spread, unlike FD which errors grow monotonically. Second, for large spreads (greater than 3.5 km in winter and 6 km in summer) the curves from neXtSIM are consistently below those from FD and getting closer to the spread. Contrarily to the previous results, the FD and *neXtSIM* models behave very differently in the summer.

The small values of the spread correspond to shorter forecast lead times (see Fig. 17) and these are the times when the *neXtSIM* model is still heavily influenced by its initial conditions of damage, as previously noted on the anisotropy ratio (Fig. 11). As the damage is irrelevant to the FD model, the initial error grows slower initially, but keeps growing while the rheology maintains the errors closer to the spread in *neXtSIM*.

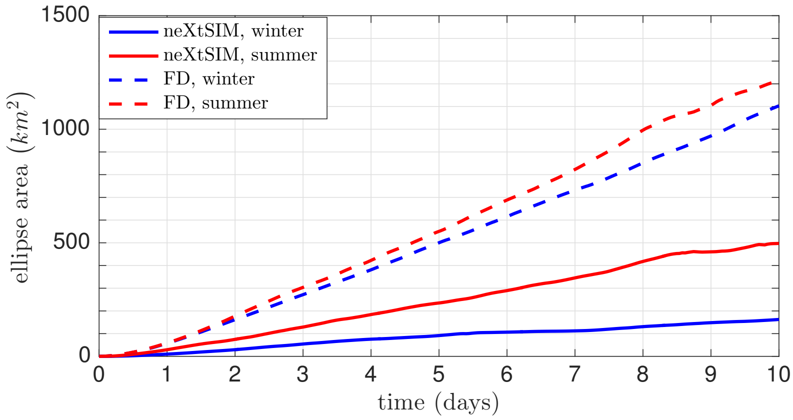

Figure 17. Time evolution of the averaged ellipse areas for *neXtSIM* (solid lines) and FD (dashed lines) in winter (blue) and in summer (red).

It should be no surprise that the two models underestimate the errors since this is a common behaviour of probabilistic forecast systems, but the differences of the shape of the spread-error relationships indicate that the two models underestimate the errors for different reasons: the *neXtSIM* ensemble is lacking spread during the initial times of the forecast but the asymptotic convergence of the spread to the errors tends to blame the constitution of the initial ensemble.

If one had considered the more linear spread-error relationship in the FD model alone, it would have been tempting to increase the variance of wind perturbation errors until a perfect match of the spread to the errors is obtained, but this would have over-tuned the variance of the wind and masked that the FD model suffers from unresolved physics.

4.4 Relevance for search and rescue operations

Whether a prediction model is too optimistic or too pessimistic may be equally problematic in view of search and rescue operations. In practice, the resources available for search and rescue operations are limited and only a given area can be covered, although the shape of the area (center and eccentricity in the case of an ellipse) may not influence the cost significantly. Thus, rather than looking at the size of the search area as estimated from the ensemble model prediction, the search-and-rescue operation can be posed as follows: for ~~an equal area that can~~ a given area to be searched, which model forecast gives the ellipse that is most likely to contain the object?

The ensemble forecast provides the expected position, $\boldsymbol{B}(t)$, and the anisotropy, $R(t)$ of the ellipse as defined previously, but the ellipse area is left free to grow homothetically from 1 km^2 to 3000 km^2. The POC increases then accordingly as the observed buoy position is more and more likely to fall within the ellipse. The dependency between the search area and the associated POC defines the so called *selectivity curve*, which makes possible a straightforward ~~models~~ model comparison: the higher the selectivity curve, the better the model's ability to locate the searched object. The selectivity curves ~~allow as also for~~

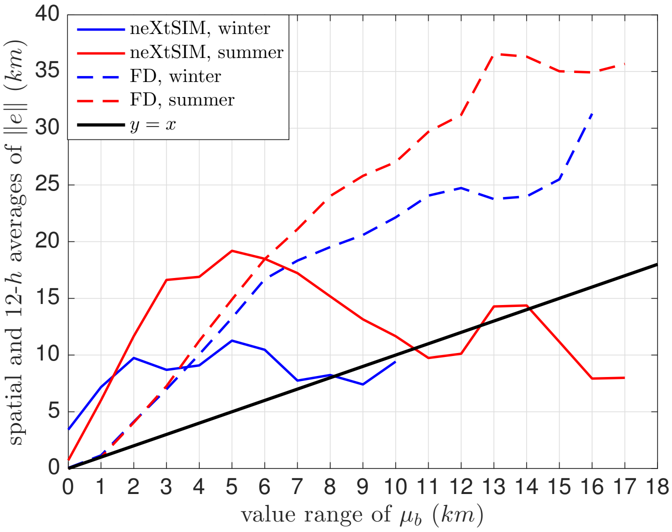

Figure 18. Spread-error relationship for 12-h averages. The curves are based on the spatial mean of the forecast error shown as a function of the spread.

also allow an immediate evaluation of the rate at which predictive skill is lost as a function of time.

For each time $t_0+\Delta t$, with $\Delta t \in \{12, 24, 36, 48, \ldots, 10\times 24\}$ hours, we compute the POC ~~, Eq. (??),~~ corresponding to search areas ranging from 1 km^2 to 3000 km^2 for both models and seasons. Results from *neXtSIM* (solid lines) and FD (dashed lines) are shown at t_0+1, 2, 3 and 7 days in Fig. 19. ~~For~~ In winter, for a given area, the POCs from *neXtSIM* are almost always above those from FD except in two cases: ~~in winter~~ at t_0+1 day ~~and~~ for search areas larger than ~~200~~ 100 km^2 ~~, and in summer at t_0+1 day~~ and at t_0+2 days for search areas ~~smaller than 7~~ larger than 500 km^2. If we neglect the anisotropy for these cases (i.e. consider circular search areas), the POCs from *neXtSIM* become larger than FD. This indicates that the strong anisotropy in *neXtSIM* is more a disadvantage for small time horizon and large search areas in this experiment. Otherwise for smaller areas, larger time horizons or in summer, considering circular or ellipsoidal search areas makes no difference (not shown). As long as the drift is longer than ~~2~~ 3 days, the selectivity curves of *neXtSIM* are systematically above FD. Whereas, in summer, for any time horizon and any POC, the results are very similar with a faint advantage to *neXtSIM*. When comparing to POCs of ellipses centered on forecasts from a deterministic *neXtSIM* run (not shown), the results are identical in winter and poorer with the deterministic run in the summer.

For both periods and both models, all curves exhibit a sigmoid shape with an inflexion point, which position depends on the time horizon (higher POC and larger search areas for longer drift duration). For a ~~7-days~~ 7 days drift in winter and a POC equal to 0.5, the area is ~~smaller than~~ around 300 km^2 with *neXtSIM*, while it reaches 1000 km^2 in FD. In the summer, a larger

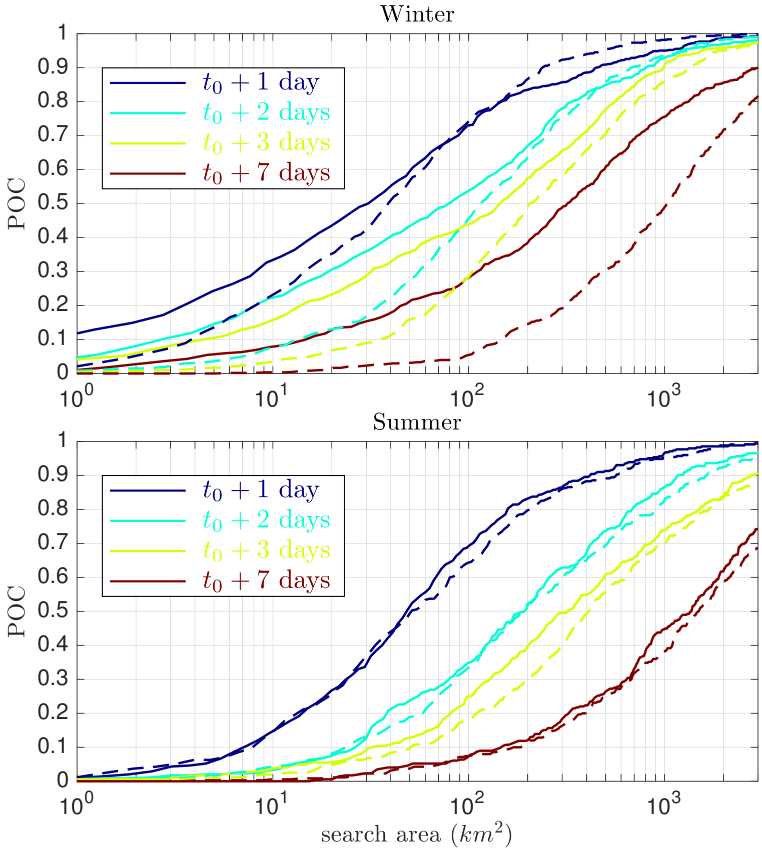

Figure 19. Time evolution of POC according to the search area for *neXtSIM* (solid lines) and FD (dashed lines) in winter (top) and in summer (bottom) for different time horizons.

area is necessary to obtain the same POC for both models. For a given search area, the gap between the POCs from *neXtSIM* and FD seems independent from the drift duration in summer, whereas in winter it increases with the time prediction horizon. It is interesting to note the lowermost value of the POC for small areas in winter, which remains above 0.1 for *neXtSIM*. This could be a consequence of the capability of *neXtSIM* to simulate immobile ice, while the FD ice is always in motion with the winds and currents.

How do the different models perform for different forecast time (i.e. drift duration)?

To answer this question, we study the time evolution of the difference between the *neXtSIM* and FD POCs: when this difference is positive/negative *neXtSIM*/FD is outperforming FD/*neXtSIM*. The POC for both models is evaluated for a fixed search area - a vertical section across the selectivity curves - equal to 50 km^2 in winter and 175 km^2 in summer, and the results are shown in Fig. (20). The chosen values of the search areas, 50 and 175 km^2, correspond to the mean ellipse areas based on the ensemble spread from *neXtSIM* after 3 days, averaged over the IABP dataset (see Fig. 17) respectively in winter and in sum-

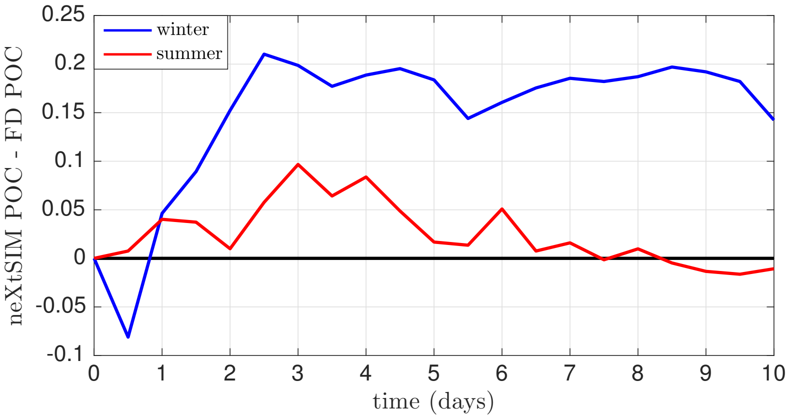

Figure 20. Time evolution of the POC difference between *neXtSIM* and FD for a search area equal to 50 km^2 in winter (blue) and equal to 175 km^2 in summer (red).

mer. Figure 20 reveals that, after 2 days in the winter, the POC of *neXtSIM* is larger ~~of~~ by about 0.2 than the POC of FD; most remarkably, such a ~~substantial~~ substantially improved skill is then maintained almost stably up to the last day of simulation (10 days). During the summer, ~~an~~ the POC of *neXtSIM* is also generally higher than the one of FD, but the difference is half of the one observed in the winter. Furthermore, after the 3rd day, the difference between the two models decreases ~~up~~ to vanish completely between day 8 and 9. The fact that most of the superiority of *neXtSIM* ~~over reveals~~ is found during winter is ~~, as stated in previous instances, in full agreement with the expectations,~~ logical and should be no surprise given that during the summer the ice mechanics in the two models ~~is similar.~~ are similar.

The negative values for lead time shorter than 1 day in winter is again likely caused by the initialization of the *neXtSIM* ensemble and another reason to constrain its initial anisotropy to observations.

5 Discussions and Conclusions

The ensemble model sensitivity experiment carried out with *neXtSIM* and with ~~a~~ an FD model reveals the prominent role of the rheology, which marks the key difference between the two models. On average over the whole Arctic *neXtSIM* is ~~35% less sensitivity~~ less sensitive to the wind perturbations than the FD, albeit large seasonal and regional differences are observed. This is exemplified by the imprint of the ice thickness field in the ensemble spread from *neXtSIM* and the much smaller sensitivity of *neXtSIM* in winter than summer, ~~contrarily~~ in contrast to the FD model (Fig. 6 and 8). Both aspects point clearly to the role of the rheology which accounts for the ice thickness and compactness. This behaviour should be expected to hold also for other sea ice rheologies than the elasto-brittle.

The two models have been tuned on ~~a common dataset of~~ different observations of ice, seen as in free drift by each model, so that the different performances originate ~~solely~~ by the differences in the resolved model physics at their best performance. The diffusion regimes of *neXtSIM* and FD are very different in winter (Fig. 13): the offset between the curves indicating differences of sensitivity, and the slopes indicating different rates of increase and thus sea ice diffusivity. The expected differences between summer and winter are only represented when the rheology is turned on.

Due to the dispersive properties of the sea ice, the shape of the ensemble of simulated buoys positions is generally anisotropic. Such anisotropy is a signature of the underlying mechanism that drives the dispersion of the members, which is the shear deformation of the ice cover along active faults/fractures in the ice. This mechanism is missing in the absence of rheology (like in the FD model) and represents a clear strength ~~and advantage of~~ in principle for the elasto-brittle rheology in *neXtSIM*~~.~~, although with the present ensemble initialization, it did not prove to be a practical advantage. Other rheological models, such as the Elasto-Viscous Plastic model, also present some degree of anisotropy (Bertino et al., 2015), although the two models have not been compared in the same conditions.

The performance of the two models differs significantly when forecasting the trajectories of IABP buoys. The ensemble mean position errors are larger in the summer (5 km after 1 day and 12.5 km after 3 days drift for *neXtSIM*, about ~~20~~16% below the FD results), and consistent with the values reported by Schweiger and Zhang (2015) (RMS errors of 6.3 km and 14 km respectively, but using different time periods). The corresponding errors are smaller in winter, especially for *neXtSIM* (~~31~~25% smaller than FD) and down to 4 km for a 1-day drift and 7.5 km for a 3-days drift. These values seem competitive compared to the year-round average RMS error of 5.1 km per day in the TOPAZ4 reanalysis (Xie et al., 2017), even though the ice drift measurements are assimilated in TOPAZ4 (Sakov et al., 2012). The RMS errors of the free drift model in Grumbine (2003) also seem to be higher than 5 km per day.

The model sensitivity to ~~winds~~ wind perturbations has been evaluated, yielding (for ~~10-days~~ 10 days drift) a spread from 5 to 10 km, for winter and summer respectively, but this is smaller than the corresponding errors (15 km from the barycentre to the observations in Fig. 15). Still, since the diffusion regime is respected (at least in the winter), we are confident that the spread simulated by the model is physically consistent. ~~Alternative sources of biases must be called~~ Other methods for perturbing the winds should be tested to remove the super-diffusive behaviour in summer however.

To futher improve the spread-error relationship, alternative sources of errors should be considered such as, for example, ~~other model inputs (~~model initial conditions and forcings (ice thickness, concentrations, damage, ocean currents). Since the errors are increasing faster in the first days of the simulations, the more likely source of local and short-term errors lies in the position and orientation of the sea ice fracture network, which is ~~not constrained at all in these experiments~~ left unconstrained in any of the experiments presented here.

Although we would expect an increase of the ensemble spread if the ice thickness, concentrations and ocean currents had been taken into account in the ensemble initialization, ~~yet~~ we do not believe it would lead to a much larger spread, especially in the winter. ~~Still it is the wind forcing being the key player in the spread evolution.~~ We suggest instead that, in the perspective of efficient sea ice forecasting, major efforts should be directed toward assimilating the observed fractures (as of satellite images). The assimilation of fracture (as objects rather than quantitative observations) represents a priori a challenging avenue in terms of data assimilation, which traditionally deals with quantitative scalar or vector observations, however we envision that the damage variable in *neXtSIM*, showing localized features, can be constrained quantitatively to deformation rates as derived from observed high-resolution ice motions and serve as "object assimilation".

In spite of the biases, the selectivity curves indicate that a probabilistic forecast using *neXtSIM* is largely more skilful than the traditional free drift model, and it has the larger potential for practical use in search and rescue operations on sea ice. Since the Arctic is not easily accessible, forecast horizons of 5 to 10 days are probably the most relevant for logistical reasons. On those time scale, the differences of POC shown in Fig. 20 indicate that the free drift model gives a poorer information in winter because of the biases in the central forecast location and the lack of anisotropy, while in the summer the use of ~~a~~ an elasto-brittle rheology is only marginally advantageous. The comparison of deterministic versus probabilistic forecast gives, as expected, an advantage to the average of the probabilistic forecast, although it is rather small and surprisingly more important in the summer, although the model non-linearities are stronger in the winter.

The physical consistency of the ensemble sensitivities is a necessary condition to the success of ensemble-based data assimilation methods (Evensen, 2009), which constitutes one of the follow-up research direction the authors are currently considering. Combining the modelling and physical novelty of *neXtSIM* with modern observations of the Arctic is seen as a major asset for forecast and reanalysis applications.

Besides the potential use of observations of fractures, as mentioned above, which is indeed another unique advantage of models such as *neXtSIM*, ice drift data are also crucial. Observations of ice drift are still seldom used for data assimilation, and when it is the case, the success is limited by the lack of sensitivity of ~~most~~ the sea ice ~~models~~ model (see, e.g. Sakov et al., 2012). Nevertheless, the main fundamental issue related to the use of data assimilation, and particularly ensemble-based ~~,~~ methods, stands in the nature of the Lagrangian mesh of *neXtSIM*, which also include the possibility of re-meshing (Rampal et al., 2016b). This feature, while essential to the skill of the model in describing the mechanics of the sea ice with great details, represents a challenge in developing compatible data assimilation schemes, as the dimension of the state space can change over time when these re-meshing occur. This problem has recently attracted attention in the data assimilation research community ~~(see, e.g. Bonan et al., 2016; Guider et al., 2017)~~ (see, e.g. Bonan et al., 2016; Guider et al., 2017; Carrassi et al., 2017) and it is also a main area of on-going investigation of the authors, following the present study.

Author contributions. The sensitivity analysis has been implemented and performed by MR. The results have been analysed by MR, PR, AC and LB. The manuscript has been written by MR and PR, then reviewed and improved with inputs from all authors.

Competing interests. The authors declare that they have no conflict of interest.

Acknowledgements. M. Rabatel, P. Rampal, A. Carrassi and L. Bertino have been ~~founded~~ funded by the Office of Naval Research project *DASIM* (award N00014-16-1-2328). P. Rampal, A. Carrassi and L. Bertino also acknowledge funding by the project *REDDA* of the Norwegian Research Council. C.K.R.T. Jones was supported by the Office of Naval Research (USA) under grants N00014-15-1-2112, and N00014-16-1-2325. The authors are grateful to J. F. Lemieux, H. Goessling and one anonymous reviewer for their insightful comments that helped improve the manuscript.

References

Abi-Zeid, I. and Frost, J. R.: SARPlan: A decision support system for Canadian Search and Rescue Operations, European Journal of Operational Research, 162, 630–653, 2005.

Bertino, L., Bergh, J., and Xie, J.: Evaluation of uncertainties by ensemble simulation, Tech. Rep. Tech. Rep. 355, NERSC, ART JIP Deliverable 3.3, Bergen, Norway, 2015.

Bonan, B., Nichols, N. K., Baines, M. J., and Partridge, D.: Data assimilation for moving mesh methods with an application to ice sheet modelling, Nonlinear Processes in Geophysics Discussions, 2016, 1–27, 2016.

Bouillon, S. and Rampal, P.: Presentation of the dynamical core of neXtSIM, a new sea ice model, Ocean Modelling, 91, 23–37, 2015a.

Bouillon, S. and Rampal, P.: On producing sea ice deformation data sets from SAR-derived sea ice motion, The Cryosphere, 9, 663–673, 2015b.

Bouillon, S., Maqueda, M., Legat, V., and Fichefet, T.: An elastic–viscous–plastic sea ice model formulated on Arakawa B and C grids, Ocean Modelling, 27, 174–184, 2009.

Breivik, Ø. and Allen, A. A.: An operational search and rescue model for the Norwegian Sea and the North Sea, Journal of Marine Systems, 69, 99–113, 2008.

Bromwich, D., Bai, L., Hines, K., hung Wang, S., Liu, Z., Lin, H.-C., hwa Kuo, Y., and Barlage, M.: Arctic System Reanalysis (ASR) Project, https://doi.org/10.5065/D6K072B5, 2012.

Buizza, R., Houtekamer, P. L., Pellerin, G., Toth, Z., Zhu, Y., and Wei, M.: A comparison of the ECMWF, MSC, and NCEP global ensemble prediction systems, Monthly Weather Review, 133, 1076–1097, 2005.

Carrassi, A., Guemas, V., Doblas-Reyes, F., Volpi, D., and Asif, M.: Sources of skill in near-term climate prediction: generating initial conditions, Climate Dynamics, 47, 3693–3712, 2016.

Carrassi, A., Bocquet, M., Bertino, L., and Evensen, G.: Data Assimilation in the Geosciences - An overview on methods, issues and perspectives, arXiv:1709.02798 [physics.ao-ph], 2017.

Coon, M., Maykut, G., Pritchard, R., Rothrock, D., and Thorndike, A.: Modeling the pack ice as an elastic-plastic material, AIDJEX Bull, 24, 1–105, 1974.

Dansereau, V.: A Maxwell-Elasto-Brittle model for the drift and deformation of sea ice, Ph.D. thesis, Laboratoire de Glaciologie et Géophysique de l'Environnement Grenoble, 2016.

Dobney, A., Klinkenberg, H., Souren, F., and Van Borm, W.: Uncertainty calculations for amount of chemical substance measurements performed by means of isotope dilution mass spectrometry as part of the PERM project, Analytica chimica acta, 420, 89–94, 2000.

Dupont, F., Higginson, S., Bourdallé-Badie, R., Lu, Y., Roy, F., Smith, G., Lemieux, J., Garric, G., and Davidson, F.: A high-resolution ocean and sea-ice modelling system for the Arctic and North Atlantic oceans, Geoscientific Model Development, 8, 1577, 2015.

Duraisamy, K. and Iaccarino, G.: Assessing turbulence sensitivity using stochastic Monte Carlo analysis, arXiv preprint, 2017.

Evensen, G.: The ensemble Kalman filter: Theoretical formulation and practical implementation, Ocean dynamics, 53, 343–367, 2003.

Evensen, G.: Data Assimilation: The Ensemble Kalman Filter, Springer-Verlag/Berlin/Heildelberg, second edn., 2009.

Gabrielski, A., Badin, G., and Kaleschke, L.: Anomalous dispersion of sea ice in the Fram Strait region, Journal of Geophysical Research: Oceans, 120, 1809–1824, 2015.

Girard, L., Weiss, J., Molines, J., Barnier, B., and Bouillon, S.: Evaluation of high-resolution sea ice models on the basis of statistical and scaling properties of Arctic sea ice drift and deformation, Journal of Geophysical Research: Oceans, 114, 2009.

Grumbine, R. W.: Virtual Floe Ice Drift Forecast Model Intercomparison*, Weather Forecast., 13, 886–890, doi:10.1175/1520-0434(1998)013<0886:VFIDFM>2.0.CO;2, 1998.

Grumbine, R. W.: Long Range Sea Ice Drift Model Verification, Tech. Rep. 3, National Centers for Environmental Prediction, Camp Springs, Maryland, 2003.

Guider, C. T., Rabatel, M., Carrassi, A., and Jones, C. K.: Data Assimilation Methods on a Non-conservative Adaptive Mesh, in: EGU General Assembly Conference Abstracts, vol. 19, p. 706, 2017.

Guitouni, A. and Masri, H.: An orienteering model for the search and rescue problem, Computational Management Science, 11, 459–473, 2014.

Hackett, B., Breivik, Ø., and Wettre, C.: Forecasting the drift of objects and substances in the ocean, pp. 507–523, Springer, 2006.

Hebert, D. A., Allard, R. A., Metzger, E. J., Posey, P. G., Preller, R. H., Wallcraft, A. J., Phelps, M. W., and Smedstad, O. M.: Short-term sea ice forecasting: An assessment of ice concentration and ice drift forecasts using the U.S. Navy's Arctic Cap Nowcast/Forecast System, J. Geophy. Res., 120, 8327–8345, doi:10.1002/ 2015JC011283., http://onlinelibrary.wiley.com/doi/10.1002/2015JC011283/abstract, 2015.

Herman, A.: Molecular-dynamics simulation of clustering processes in sea-ice floes, Physical Review E., 84, 2011.

Hibler III, W. D.: A dynamic thermodynamic sea ice model, Journal of Physical Oceanography, 9, 815–846, 1979.

Hopkins, M. A., Frankenstein, S., and Thorndike, A. S.: Formation of an aggregate scale in Arctic sea ice, Journal of Geophysical Research: Oceans, 109, 2004.

Hunke, E. C. and Dukowicz, J. K.: An elastic–viscous–plastic model for sea ice dynamics, Journal of Physical Oceanography, 27, 1849–1867, 1997.

Kwok, R.: Near zero replenishment of the Arctic multiyear sea ice cover at the end of 2005 summer, Geophysical Research Letters, 34, 2007.

Lavergne, T. and Eastwood, S.: Low resolution sea ice drift Product User's Manual - v1.7., Tech. rep., SAF/OSI/CDOP/met.no/TEC/MA/128, EUMETSAT OSI SAF - Ocean and Sea Ice Satellite Application Facility, www.osi-saf.org, 2015.

Leith, C. E.: Theoretical skill of Monte Carlo forecasts, Monthly Weather Review, 102, 409–418, 1974.

Lemieux, J.-F., Tremblay, B. L., Dupont, F., Plante, M., Smith, G. C., and Dumont, D.: A basal stress parameterization for modeling landfast ice, Journal of Geophysical Research: Oceans, 120, 3157–3173, 2015.

Lemieux, J. F., Beaudoin, C., Dupont, F., Roy, F., Smith, G. C., Shlyaeva, A., Buehner, M., Caya, A., Chen, J., Carrieres, T., Pogson, L., Derepentigny, P., Plante, A., Pestieau, P., Pellerin, P., Ritchie, H., Garric, G., and Ferry, N.: The Regional Ice Prediction System (RIPS): Verification of forecast sea ice concentration, Q. J. R. Meteorol. Soc., 142, 632–643, doi:10.1002/qj.2526, 2016.

Leppäranta, M.: The drift of sea ice, Springer Science & Business Media, second edition edn., 2011.

Leutbecher, M. and Palmer, T. N.: Ensemble forecasting, Journal of Computational Physics, 227, 3515–3539, 2008.

Lukovich, J. V., Hutchings, J. K., and Barber, D. G.: On sea-ice dynamical regimes in the Arctic Ocean, Annals of Glaciology, 56, 323–331, 2015.

Maio, A. D., Martin, M. V., and Sorgente, R.: Evaluation of the search and rescue LEEWAY model in the Tyrrhenian Sea: a new point of view, Natural Hazards and Earth System Sciences, 16, 1979–1997, 2016.

Marsan, D., Stern, H., Lindsay, R., and Weiss, J.: Scale Dependence and Localization of the Deformation of Arctic Sea Ice, Physical Review Letters, 93, 178 501, 2004.

Melsom, A., Counillon, F., LaCasce, J. H., and Bertino, L.: Forecasting search areas using ensemble ocean circulation modeling, Ocean Dynamics, 62, 1245–1257, 2012.

Molteni, F., Buizza, R., Palmer, T. N., and Petroliagis, T.: The ECMWF ensemble prediction system: Methodology and validation, Quarterly journal of the royal meteorological society, 122, 73–119, 1996.

Motra, H. B., Hildebrand, J., and Wuttke, F.: The Monte Carlo Method for evaluating measurement uncertainty: Application for determining the properties of materials, Probabilistic Engineering Mechanics, 45, 220–228, 2016.

Poulain, P. M. and Niiler, P. P.: Statistical-Analysis of the Surface Circulation in the California Current System Using Satellite-Tracked Drifters, Journal of Physical Oceanography, 19, 1588–1603, 1989.

Rabatel, M., Labbé, S., and Weiss, J.: Dynamics of an assembly of rigid ice floes, Journal of Geophysical Research: Oceans, 120, 5887–5909, 2015.

Rabatel, M., Rampal, P., Bertino, L., Carrassi, A., and Jones, C. K.: Sensitivity Analysis of a Lagrangian Sea Ice Model, in: EGU General Assembly Conference Abstracts, vol. 19, p. 688, 2017.

Rampal, P., Weiss, J., Marsan, D., Lindsay, R., and Stern, H.: Scaling properties of sea ice deformation from buoy dispersion analysis, Journal of Geophysical Research, 113, C03 002, 2008.

Rampal, P., Weiss, J., Marsan, D., and Bourgoin, M.: Arctic sea ice velocity field: general circulation and turbulent-like fluctuations, J. Geophys. Res., 114, 2009.

Rampal, P., Weiss, J., Dubois, C., and Campin, J. M.: IPCC climate models de not capture Arctic sea ice drift acceleration: Consequences in terms of projected sea ice thinning and decline, J. Geophys. Res., 116, 2011.

Rampal, P., Bouillon, S., Bergh, J., and Ólason, E.: Arctic sea-ice diffusion from observed and simulated Lagrangian trajectories, The Cryosphere, 10, 1513–1527, 2016a.

Rampal, P., Bouillon, S., Ólason, E., and Morlighem, M.: neXtSIM: A new Lagrangian sea ice model, The Cryosphere, 10, 1055–1073, 2016b.

Rigor, I.: IABP Drifting Buoy Pressure, Temperature, Position, and Interpolated Ice Velocity, Version 1. Subset C. Compiled by Polar Science Center. Boulder, Colorado USA. NSIDC: National Snow and Ice Data Center., doi:10.7265/N53X84K7, 2002.

Sakov, P., Counillon, F., Bertino, L., Lisaeter, K. A., Oke, P. R., and Korablev, A.: TOPAZ4: an ocean-sea ice data assimilation system for the North Atlantic and Arctic, Ocean Sci., 8, 633–656, 2012.

Schweiger, A. J. and Zhang, J.: Accuracy of short-term sea ice drift forecasts using a coupled ice-ocean model, Journal of Geophysical Research: Oceans, 120, 7827–7841, doi:10.1002/2015JC011273, http://dx.doi.org/10.1002/2015JC011273, 2015.

Semtner, A. J.: A Model for the Thermodynamic Growth of Sea Ice in Numerical Investigations of Climate, Journal of Physical Oceanography, 6, 379–389, 1976.

Smith, G. C., Roy, F., Reszka, M., Surcel Colan, D., He, Z., Deacu, D., Belanger, J.-M., Skachko, S., Liu, Y., Dupont, F., Lemieux, J.-F., Beaudoin, C., Tranchant, B., Drévillon, M., Garric, G., Testut, C.-E., Lellouche, J.-M., Pellerin, P., Ritchie, H., Lu, Y., Davidson, F., Buehner, M., Caya, A., and Lajoie, M.: Sea ice Forecast Verification in the Canadian Global Ice Ocean Prediction System, Q. J. R. Meteorol. Soc., pp. n/a–n/a, doi:10.1002/qj.2555, http://doi.wiley.com/10.1002/qj.2555, 2015.

Stroeve, J., Holland, M. M., Meier, W., Scambos, T., and Serreze, M. C.: Arctic sea ice decline: Faster than forecast, Geophys. Res. Lett., 34, 2007.

Stroeve, J. C., Serreze, M. C., Holland, M. M., Kay, J. E., Malanik, J., and Barrett, A. P.: The Arctic's rapidly shrinking sea ice cover: a research synthesis, Clim. Change, 110, 1005–1027, 2012.

Taylor, G. I.: Diffusion by continuous movements, Proceedings of the London Mathematical Society, 20, 196–211, 1921.

Thorndike, A. S. and Colony, R.: Sea ice motion in response to geostrophic winds, Journal of Geophysical Research: Oceans, 87, 5845–5852, 1982.

Weiss, J. and Schulson, E. M.: Coulombic faulting from the grain scale to the geophysical scale: lessons from ice, Journal of Physics D: Applied Physics, 42, 214 017, 2009.

Weiss, J., Schulson, E. M., and Stern, H. L.: Sea ice rheology from in-situ, satellite and laboratory observations: Fracture and friction, Earth and Planetary Science Letters, 255, 1–8, 2007.

Wilchinsky, A. V., Feltham, D. L., and Hopkins, M. A.: Effect of shear rupture on aggregate scale formation in sea ice, Journal of Geophysical Research: Oceans, 115, 2010.

Williams, K. D., Harris, C. M., Bodas-Salcedo, A., Camp, J., Comer, R. E., Copsey, D., Fereday, D., Graham, T., Hill, R., Hinton, T., Hyder, P., Ineson, S., Masato, G., Milton, S. F., Roberts, M. J., Rowell, D. P., Sanchez, C., Shelly, A., Sinha, B., Walters, D. N., West, A., Woollings, T., and Xavier, P. K.: The Met Office Global Coupled model 2.0 (GC2) configuration, Geoscientific Model Development, 8, 1509–1524, doi:10.5194/gmd-8-1509-2015, http://www.geosci-model-dev.net/8/1509/2015/, 2015.

Xie, J., Bertino, L., Counillon, F., Lisæter, K. A., and Sakov, P.: Quality assessment of the TOPAZ4 reanalysis in the Arctic over the period 1991-2013, Ocean Science, 13, 123, 2017.

Zhang, H., Prater, M. D., and Rossby, T.: Isopycnal Lagrangian statistics from the North Atlantic Current RAFOS float observations, Journal of Geophysical Research: Oceans, 106, 13 817–13 836, 2001.

Zhu, Y.: Ensemble forecast: A new approach to uncertainty and predictability, Advances in atmospheric sciences, 22, 781–788, 2005.